Computational modeling of precipitation and metal oxidation

Youhai Wen, Jeffrey Hawk, David Alman

ORD, NETL

April 27-30, 2015

Acknowledgements

- **Strategic Center for Coal, NETL for supporting this ORD activity through the IPT Program.**
  - Robert Romanosky (Technology Manager)
  - Charles Miller (Project Monitor)
  - Vito Cedro (SCC)
- **Tianle Cheng (ORISE postdoc)**

IPT Task 3.4: Computational Aspects in Alloy Design & Life Prediction

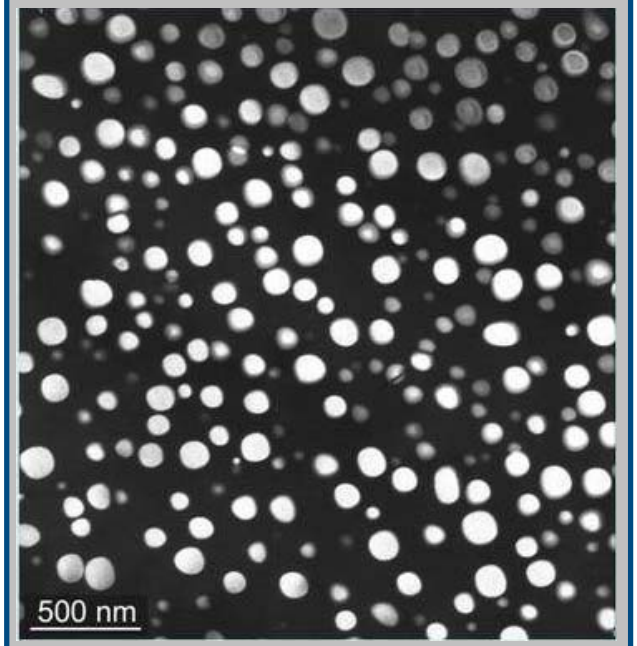

Precipitation

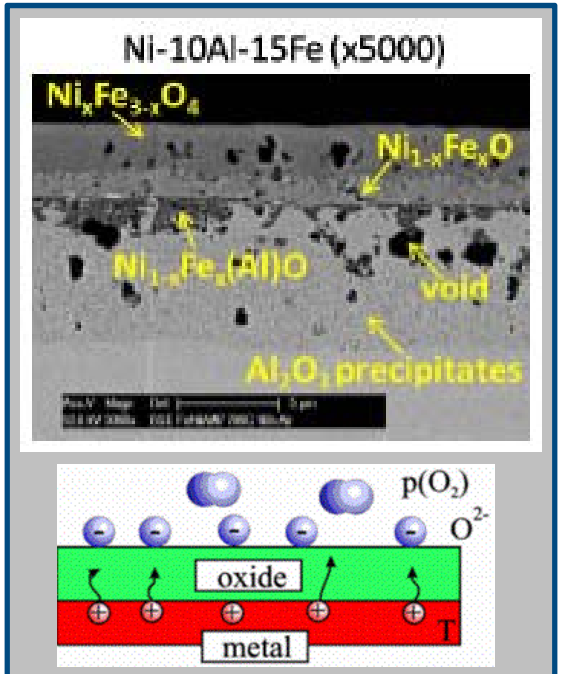

Metal Oxidation

Matrix Strength

Surface Attack

NETL Microstructural Stability Focused Areas of Modeling

Subtask 1: Precipitation kinetics modeling

205 C/min **24 C/min**

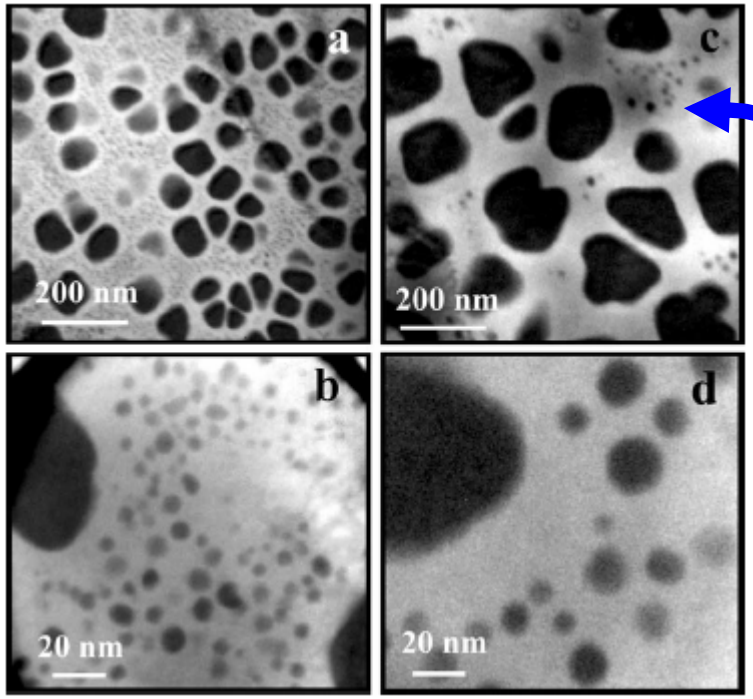

Rene 88DT Disk Alloy

G.B.Viswanathan, et al Acta mater. 2005

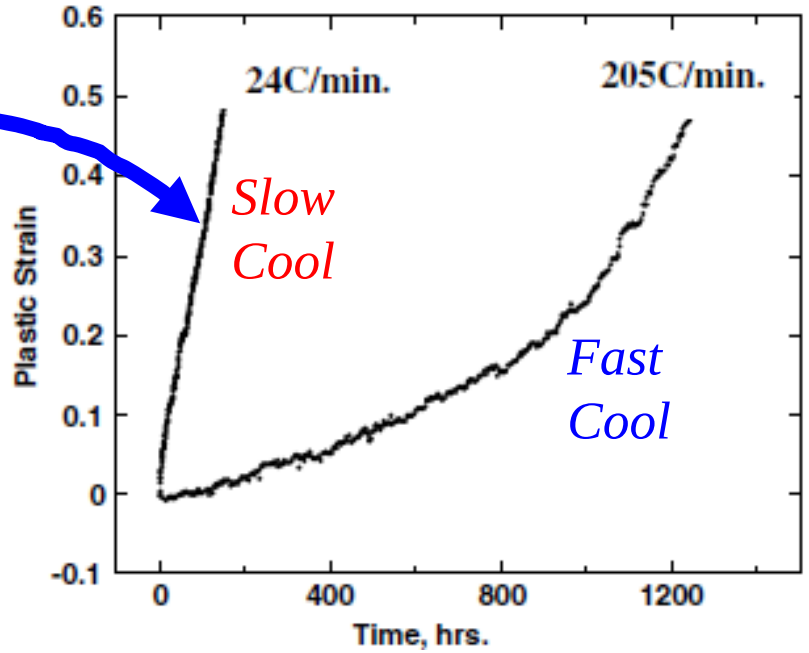

Creep Rate comparison (650C, 838 MPa)

Microstructure and Performance

The Precipitation Modeling

Goal: Develop an engineering tool that can predict precipitation process under representative thermomechanical processing and service conditions

The Challenges

- **High volume fraction of precipitates excluding any analytical solutions**
- **Complex thermal heat treating & thermo mechanical service condition**
- **Multi-component & multi-phase**

Phase-field method has the potential

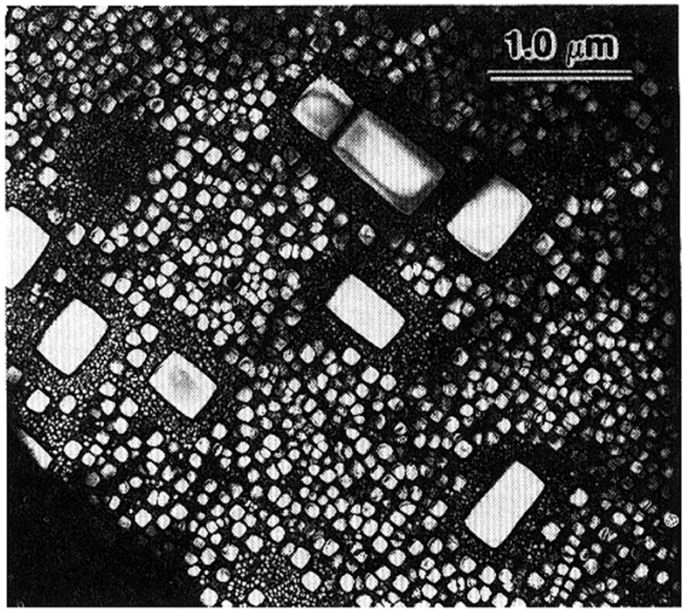

M.E. Gurtin and P.W. Voorhees.

NETL Multi-Component Phase-Field Precipitation Model

- **1D, 2D, and 3D capability**
- **Multi-Component: 7 components in present work**
- **Two phases: γ and γ' in Ni-base superalloys**
- **Direct link to CALPHAD Database: PanEngine from CompuTherm**

Haynes 282 Precipitation Kinetics

Baseline alloy ⟷

	Al	Co	Cr	Fe	Mo	Ti	Ni	Vol.%
1	1.5	10.0	20.0	1.5	8.5	2.1	Bal	18.86
2	**1.8**	10.0	20.0	1.5	8.5	2.1	Bal	21.08
3	1.5	**11.0**	20.0	1.5	8.5	2.1	Bal	18.91
4	1.5	10.0	**21.0**	1.5	8.5	2.1	Bal	18.97
5	1.5	10.0	20.0	1.5	**9.5**	2.1	Bal	19.05
6	1.5	10.0	20.0	1.5	8.5	**2.5**	Bal	21.62

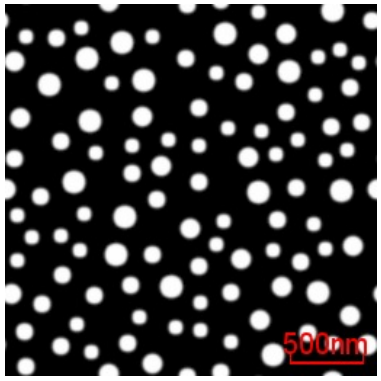

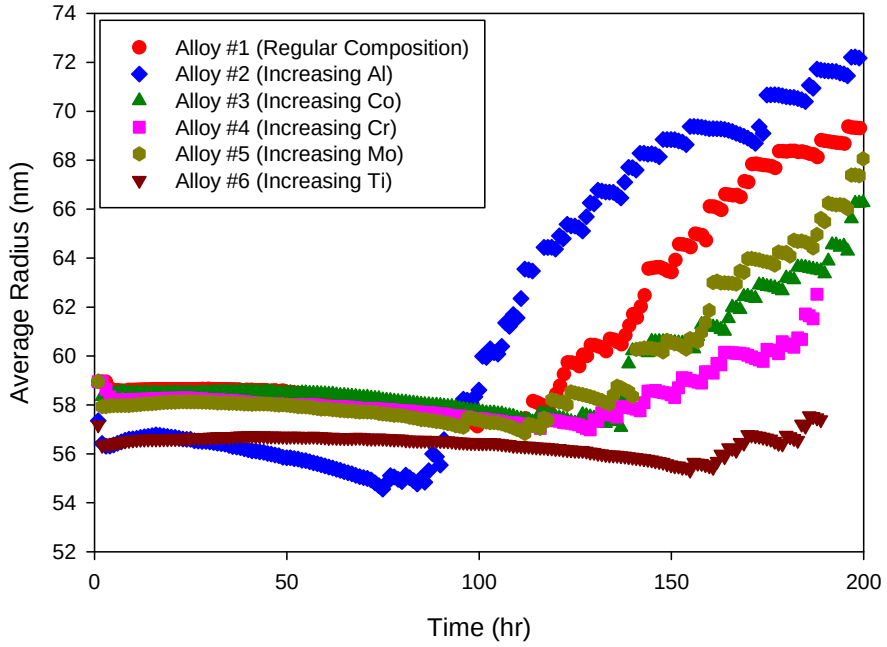

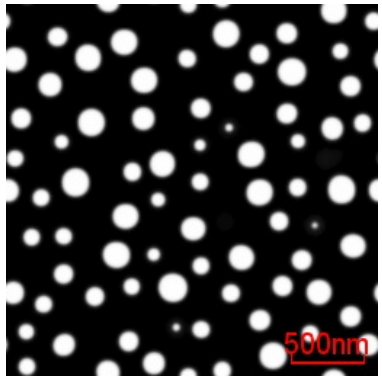

Developing a Virtual Tool for Alloy Chemistry Screening

Precipitation Kinetics Model Validation

Aged at 760°C for 0 to 10,000 hrs , Water Quenched, gamma prime size examined by TEM
(20,000 hr sample on-going)

Alloy	Ni	Cr	Co	Mo	Ti	Al	Ti/Al	k
Nominal	Bal	18.5-20.5	9-11	8-9	1.9-2.3	1.38-1.65		
H282-B	Bal	19.22	9.86	8.49	1.94	1.54	1.25	0.38
H282-C	Bal	19.19	9.85	8.50	2.22	1.27	1.75	0.35

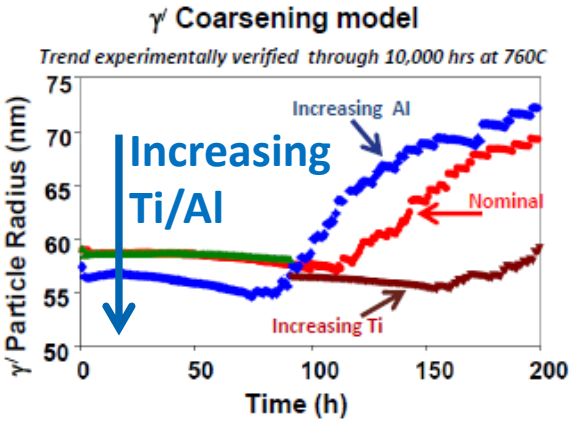

Coarsening Rate, k

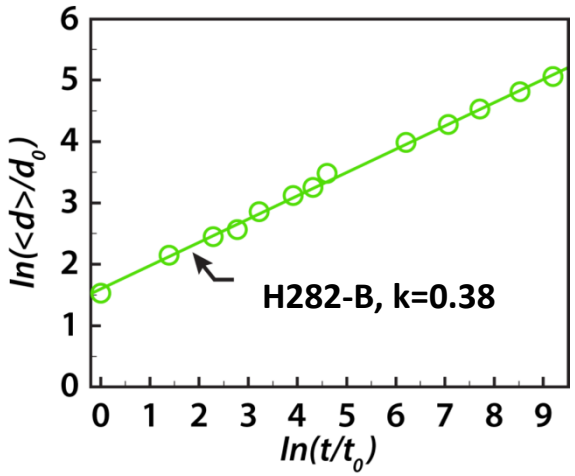

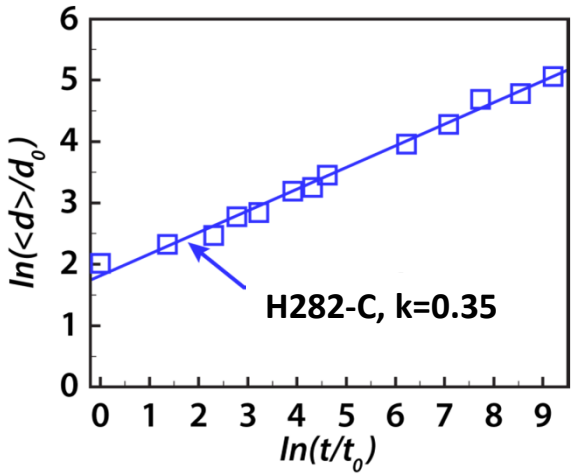

Model predicts higher Ti/Al ratio retards gamma prime coarsening rate
Model experimentally verified

Wen, Cheng, Jablonski, Sears, and Hawk, Proceedings of 8th Inter. Symp. on Superalloy 718 & Derivatives, 2014

Summary of Precipitation Modeling Task

- Developed a multicomponent Phase-Field model that can simulate precipitation kinetics in Ni-based commercial alloys
- Demonstrated that this model has the potential to be used for composition screening for a more stable precipitation microstructure
- Preliminary validation is promising

Subtask 2: Metal Oxidation Modeling

The Goal

Develop a modeling toolbox to link material's operating environment to its performance

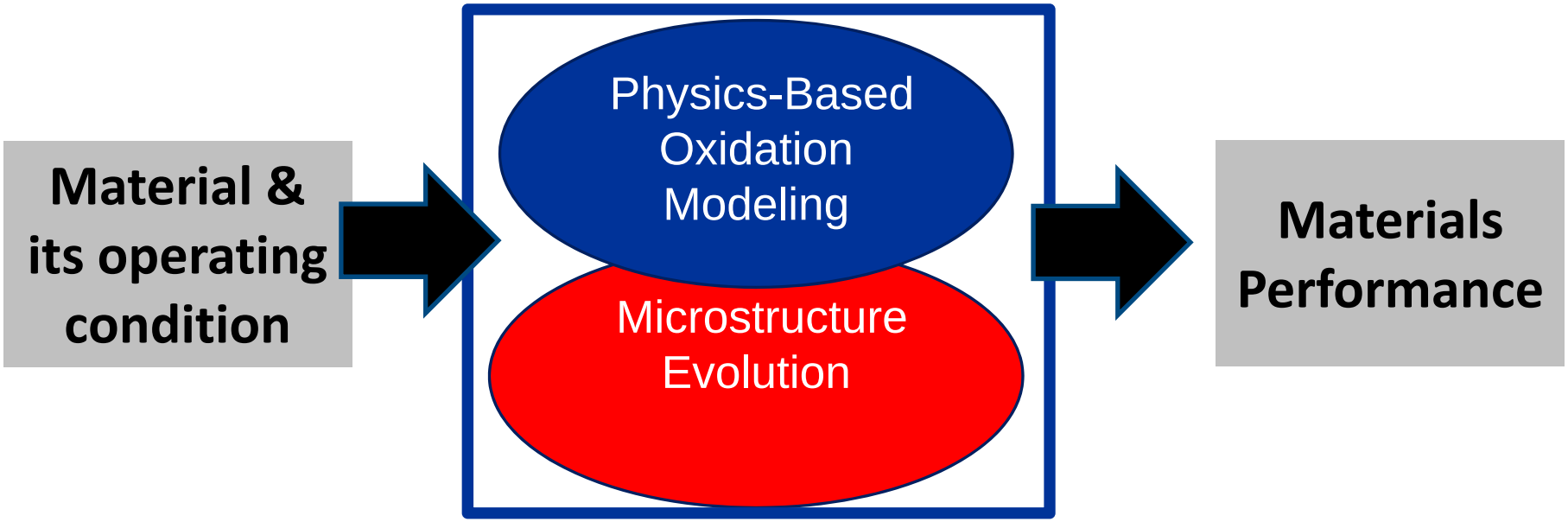

Metal Oxidation Modeling

Cabrera -Mott Theory

Moderate film thickness

Wagner Theory

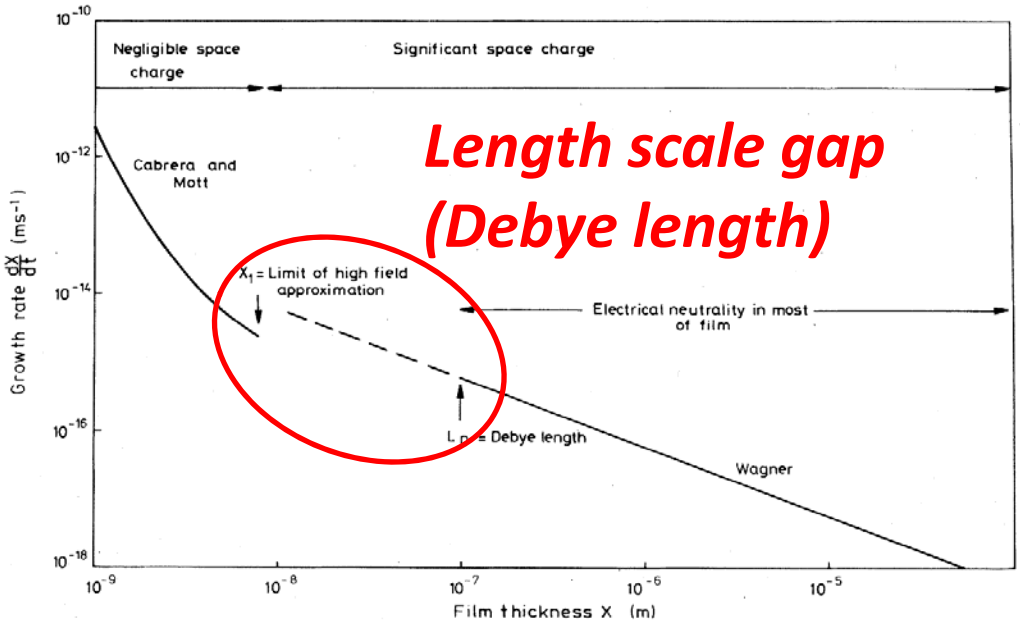

(Atkinson, *Review of Modern Physics*, 1985)

***Moderate film thickness regime*:**

The coupling of charge interaction, ionic diffusion, and chemical reaction has to be addressed.

Phase-field Modeling of Oxidation with Charge Interaction

To describe the three phases involved:

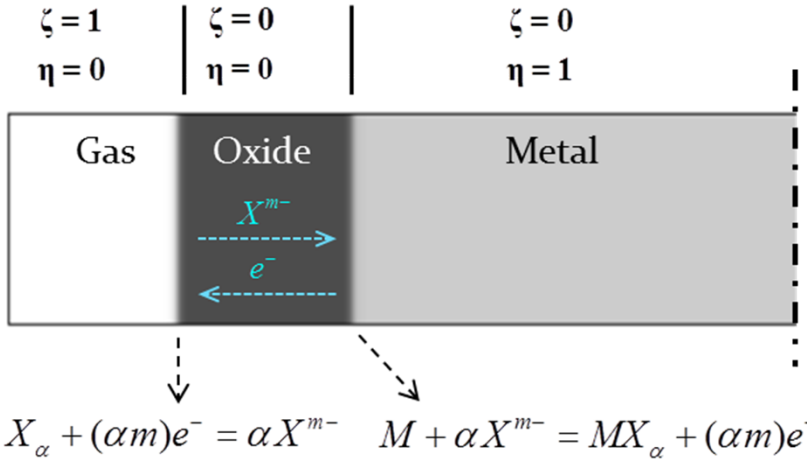

Symmetric

$$\frac{d[X^-]}{dt} = k_I p_X \left([X^-]^* - [X^-]\right)[e^-] \qquad \frac{d[X^-]}{dt} = \frac{d[M]}{dt} = -k_{II}[M][X^-]$$

$$\frac{d[e^-]}{dt} = -k_I p_X \left([X^-]^* - [X^-]\right)[e^-] \qquad \frac{d[e^-]}{dt} = k_{II}[M][X^-]$$

To describe the compositional profiles:

C1 --- Oxidant composition

C2 --- Electron composition

C3 --- Positive charges, i.e. electron holes /point defect

Governing Equations

[X^-]: $$\frac{\partial c_1}{\partial t} = K_I \Lambda_\zeta (Q\tilde{c}_2 - \tilde{c}_1) - K_{II}\Lambda_\eta \tilde{c}_1 + \nabla\cdot(\tilde{D}_1 \nabla \tilde{c}_1) - \frac{e}{k_B T}\nabla\cdot(D_1 c_1 z_1 \mathbf{E})$$

[e^-]: $$\frac{\partial c_2}{\partial t} = -K_I \Lambda_\zeta (Q\tilde{c}_2 - \tilde{c}_1) + K_{II}\Lambda_\eta \tilde{c}_1 + \nabla\cdot(\tilde{D}_2 \nabla \tilde{c}_2) - \frac{e}{k_B T}\nabla\cdot(D_2 c_2 z_2 \mathbf{E})$$

[c^+]: $$\frac{\partial c_3}{\partial t} = \nabla\cdot(D_3 \nabla c_3) - \frac{e}{k_B T}\nabla\cdot(D_3 c_3 z_3 \mathbf{E})$$

[M]: $$\frac{\partial \eta}{\partial t} = -K_V K_{II}\Lambda_\eta \tilde{c}_1 + M_\eta \nabla^2\left(\partial f / \partial \eta - \beta \nabla^2 \eta\right)$$

Governing Equations

Reaction | Diffusion + Electromigration

[X⁻]: $$\frac{\partial c_1}{\partial t} = K_I \Lambda_\zeta (Q\tilde{c}_2 - \tilde{c}_1) - K_{II}\Lambda_\eta \tilde{c}_1 + \nabla\cdot(\tilde{D}_1 \nabla \tilde{c}_1) - \frac{e}{k_B T}\nabla\cdot(D_1 c_1 z_1 \mathbf{E})$$

[e⁻]: $$\frac{\partial c_2}{\partial t} = -K_I \Lambda_\zeta (Q\tilde{c}_2 - \tilde{c}_1) + K_{II}\Lambda_\eta \tilde{c}_1 + \nabla\cdot(\tilde{D}_2 \nabla \tilde{c}_2) - \frac{e}{k_B T}\nabla\cdot(D_2 c_2 z_2 \mathbf{E})$$

[c⁺]: $$\frac{\partial c_3}{\partial t} = \nabla\cdot(D_3 \nabla c_3) - \frac{e}{k_B T}\nabla\cdot(D_3 c_3 z_3 \mathbf{E})$$

[M]: $$\frac{\partial \eta}{\partial t} = -K_V K_{II}\Lambda_\eta \tilde{c}_1 + M_\eta \nabla^2\left(\partial f / \partial \eta - \beta \nabla^2 \eta\right)$$

$\tilde{c}_i = [1 + \kappa_G p(\zeta) + \kappa_M{}^{(i)} p(\eta)] c_i$ Equivalent concentration

$\Lambda_\eta = \eta^p (1-\eta)^q$, $\Lambda_\xi = \xi^p (1-\xi)^q$ Locator functions

$F(\eta) = \int \left[f(\eta) + \frac{1}{2}\beta |\nabla \eta|^2 \right] dV$ Equilibrium free energy with respect to η

The electric field, satisfying Poisson's equation, is solved by **an efficient numerical scheme** for arbitrary **dielectric heterogeneity**

$$\nabla\cdot[\varepsilon(\mathbf{r})\nabla\varphi(\mathbf{r})] + \rho_f(\mathbf{r}) = 0$$

Linear-Parabolic Transition in Kinetics

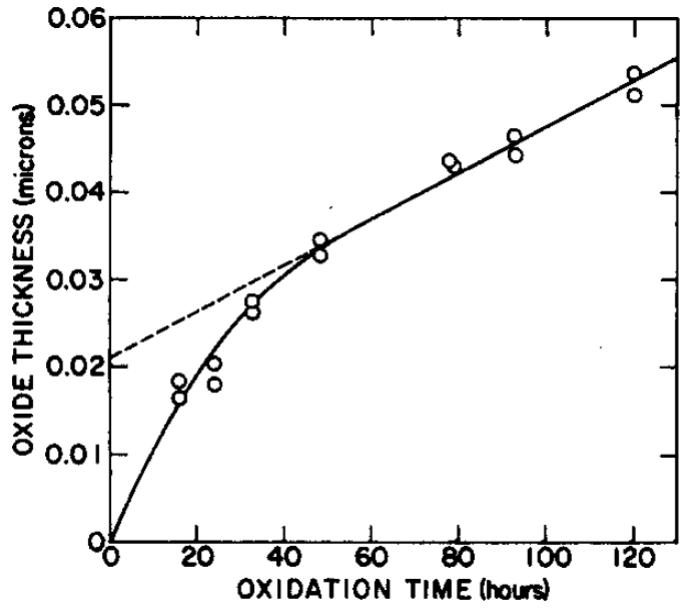

FIG. 6. Oxidation of silicon in dry oxygen at 700°C.

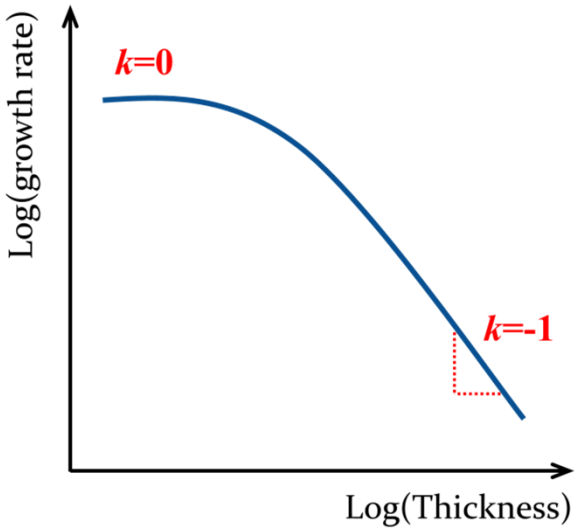

(expected plot on a log-log plot)

Deal & Grove, J.A.P. 1965: assume steady state diffusion, without considering electric field

Can we capture the transition without any *a prior* assumptions?

Multiscale Simulation: Linear-Parabolic Transition

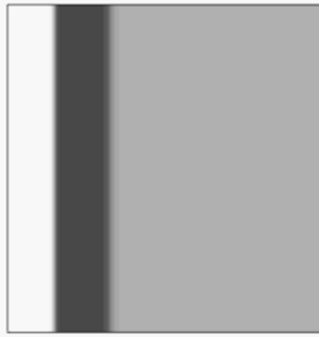

❖ Reproducing classical Deal-Grove reaction-diffusion model (analytical) with explicit consideration of charge transport

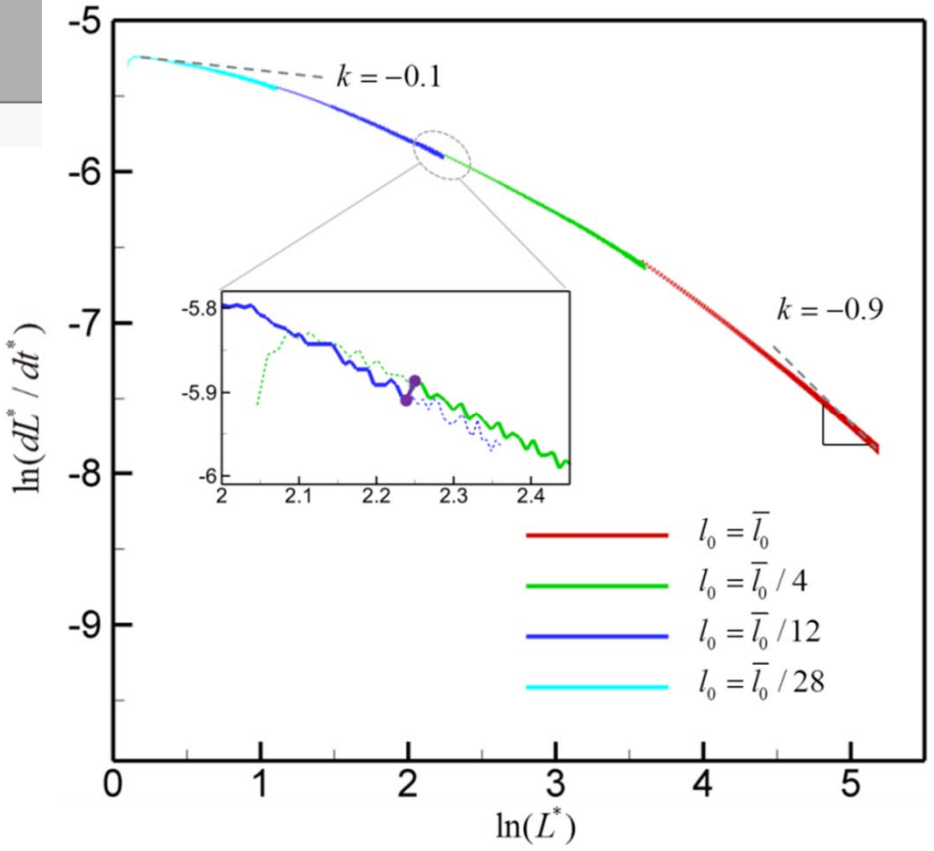

- **Continuous linear to parabolic transition**
- **Four different simulations at 4 length scales are combined together**
- **Resemble 'relay-race game' in track and field**
- **Excellent agreements at the "exchange of baton" zones**

Cheng, Wen, Hawk, J. Phys. Chem. C 118(2014), 1269-1284

Multiscale Simulation: Linear-Parabolic Transition

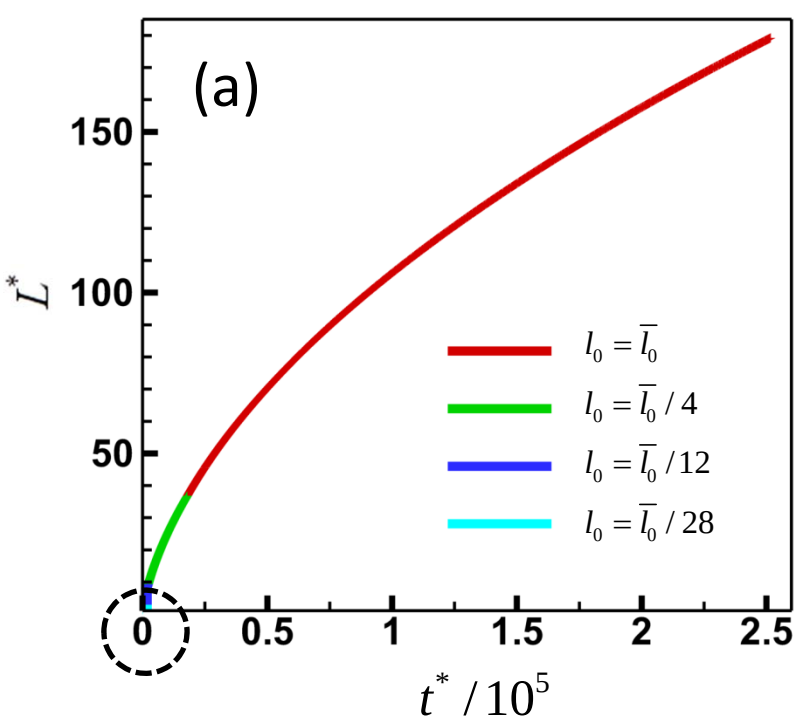

Overall growth kinetics

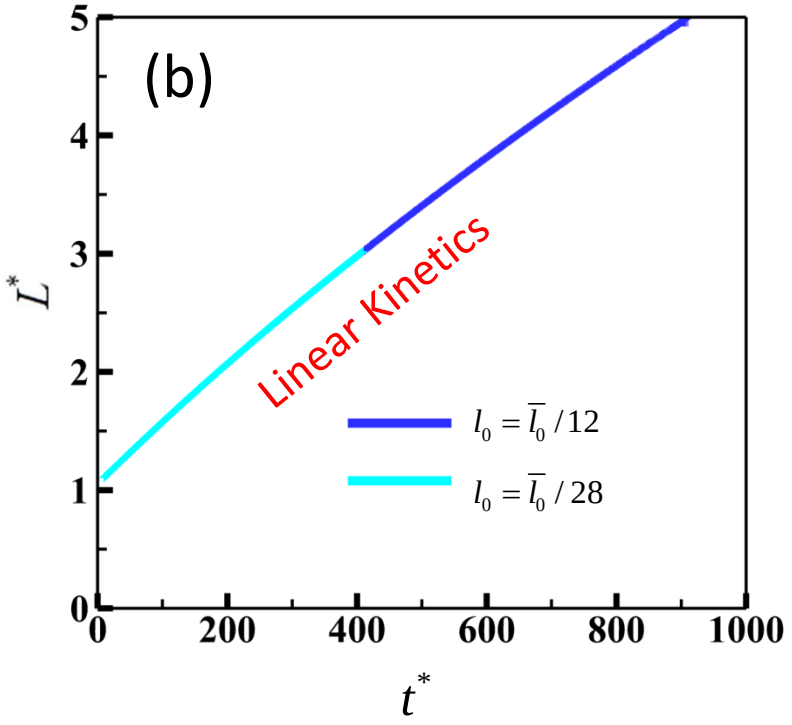

Initial stage growth kinetics

Ion concentrations, space charge density, electric field and potential distribution at representative stages

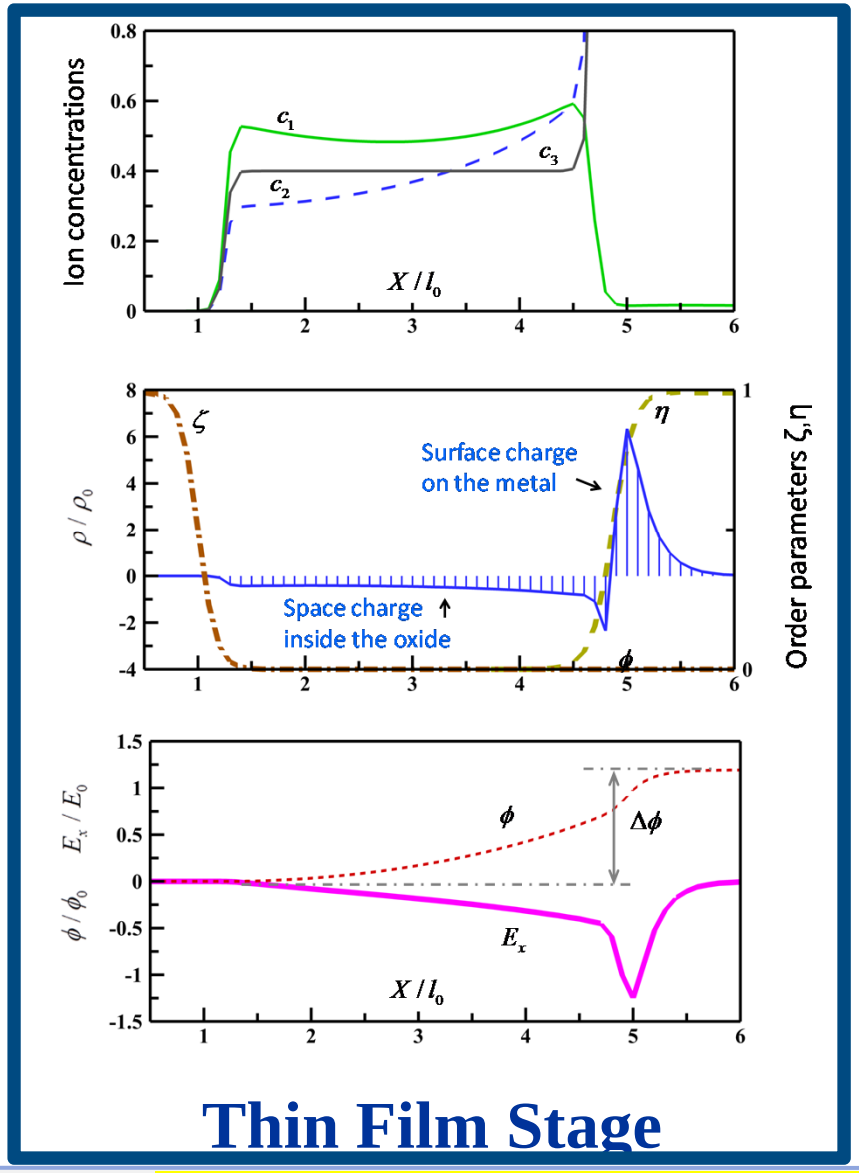

Thin Film Stage

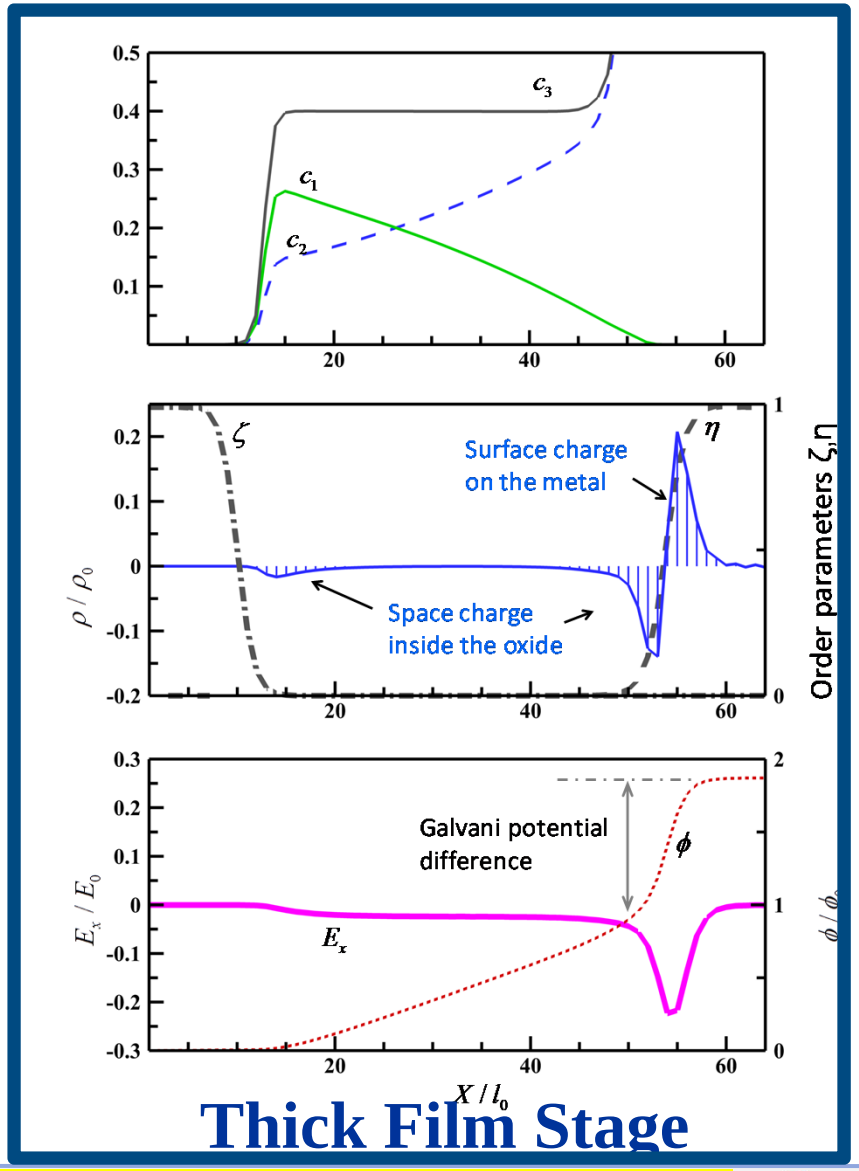

Thick Film Stage

Cheng, Wen, Hawk, J. Phys. Chem. C 118(2014), 1269-1284

Simulated Film Growth Rate with Increasing Thickness

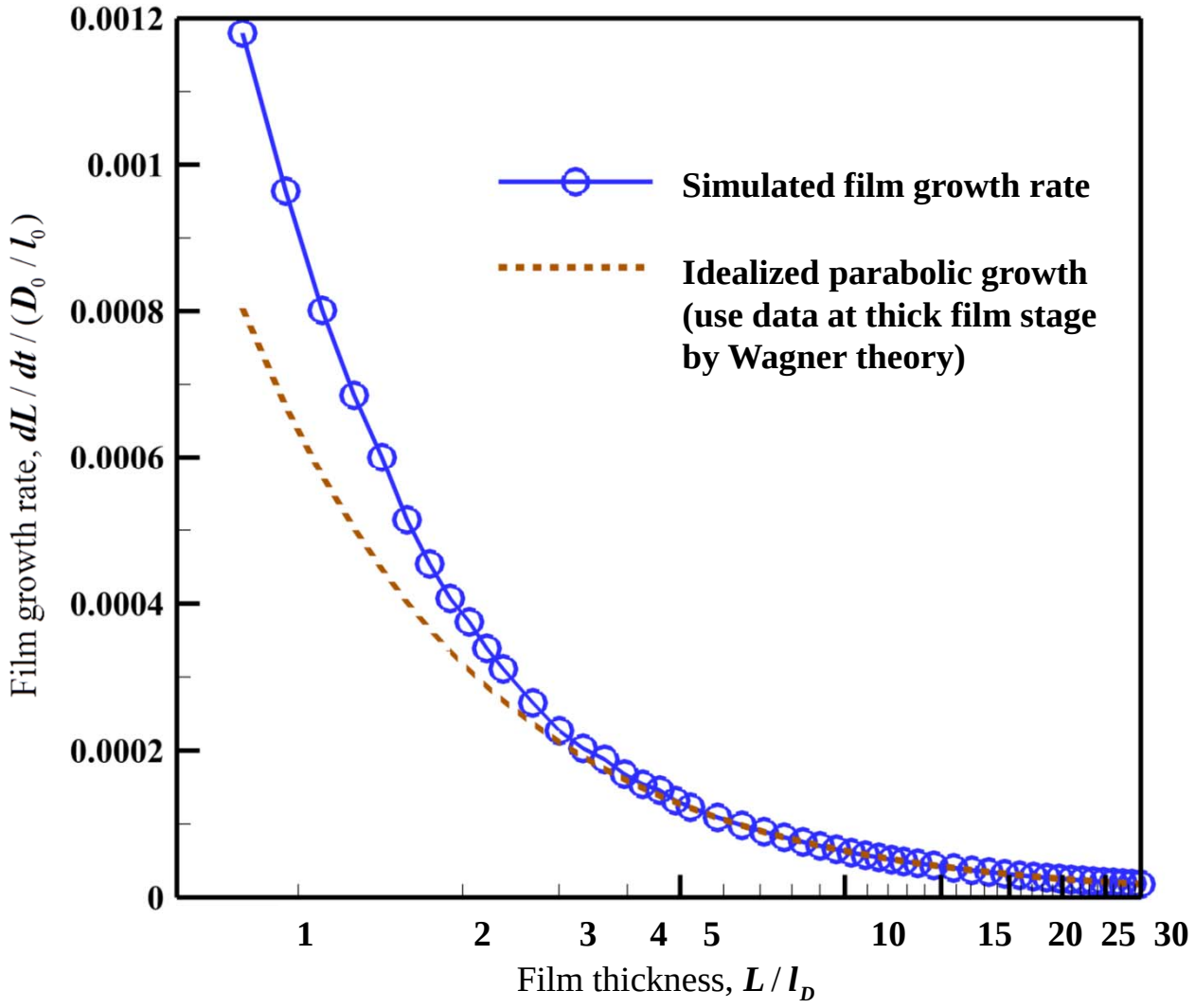

Space charge effect can not be ignored

Some confusion about Wagner's theory

Two key assumptions in Wagner's theory:

- Coupled-currents condition
- Local thermodynamic equilibrium

Fromhold challenged the self-consistency of Wagner's theory by stating that the electric field deduced from the 'coupled-currents condition' contradicts the **electrochemical Gibbs-Duhem relation**. (Fromhold et al, *J. Phys. Soc. Jpn*, 1973)

- Local equilibrium is violated?
- Wagner's theory is not self-consistent?

Does the local equilibrium assumption contradict the kinetics constrained by the coupled-currents condition?

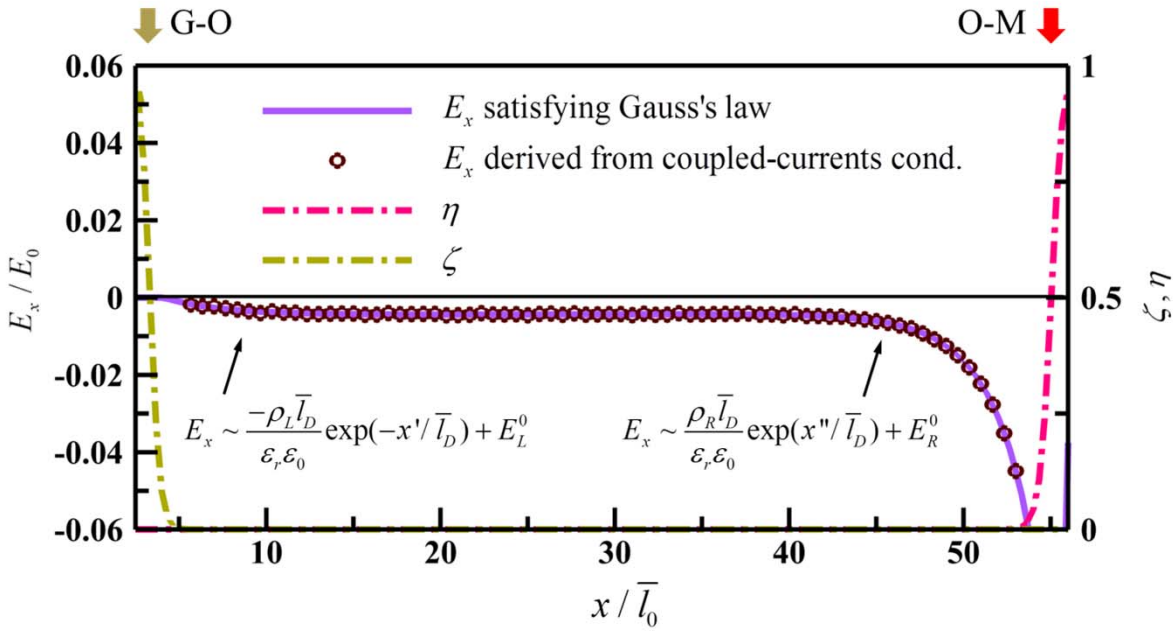

- **Local equilibrium is also assumed in our model**
- **Coupled-currents condition is verified to be satisfied.**

Cheng, Wen, Hawk, *J. Phys. Chem. C*, 2014

Does the local equilibrium assumption contradict the kinetics constrained by the coupled-currents condition? No

Local equilibrium -> Electrochemical Gibbs-Duhem relation $\sum_i c_i \nabla \bar{\mu}_i = \nabla p$

$\nabla p = 0$ **Is assumed in Fromhold's derivation and classical Wagner theory**

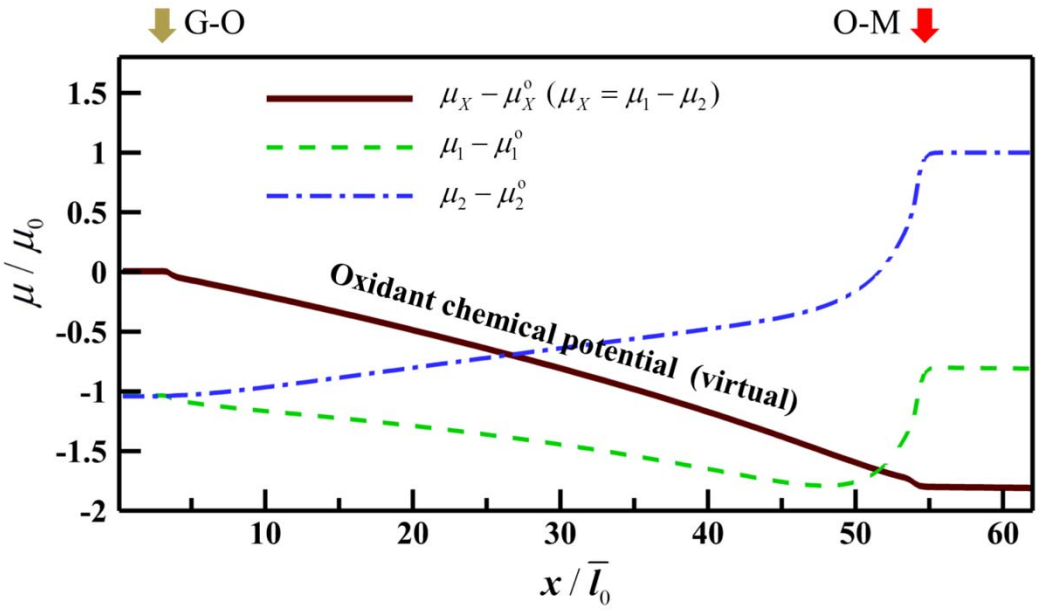

Cheng, Wen, Hawk, *J. Phys. Chem. C*, 2014

Gradient of the virtual chemical potential of oxygen indicates $\nabla p \neq 0$

$\nabla p \neq 0$ **due to non-stoichiometry of the oxide and the gradients of total point defects density**

Electric Field in a Growing Oxide Film

Two dominant representations:

- Homogeneous electric field across the film
- Electric field decays to zero exponentially away from the surface/interface assuming thermodynamic equilibrium

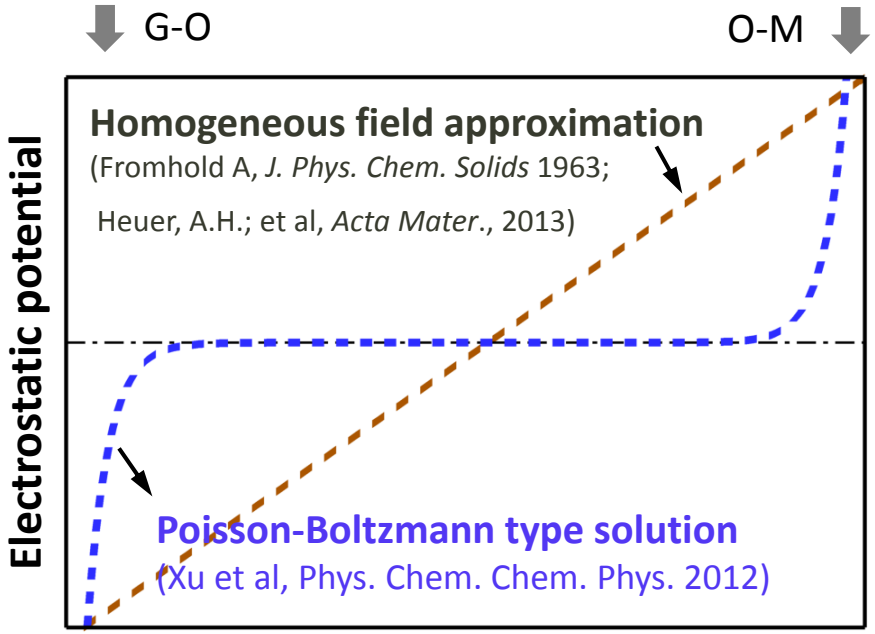

Kinetics is missing!

Electric Field in a Growing Oxide Film

Two dominant representations:

- Homogeneous electric field across the film
- Electric field decays to zero exponentially away from the surface/interface assuming thermodynamic equilibrium

$$J_i = -D_i \nabla c_i + \varpi_i \mathbf{E} c_i \quad \text{Flux equations}$$

$$\varepsilon \nabla \bullet \mathbf{E} = \sum_i z_i e N_A c_i \quad \text{Linearized Poisson Boltzmann}$$

- Two negatively charged transporting species with identical valences (i.e. z1=z2=-1), e.g. electrons and interstitial anions
- Assume coupled-current condition

$$E = Ae^{-x/l_D} + E^o$$

$$E^o = \frac{k_B T}{e\bar{c}} \frac{D_1 - D_2}{D_1 D_2} J^o$$

$$l_D = \sqrt{\varepsilon k_B T / N_A e^2 \bar{c}}$$

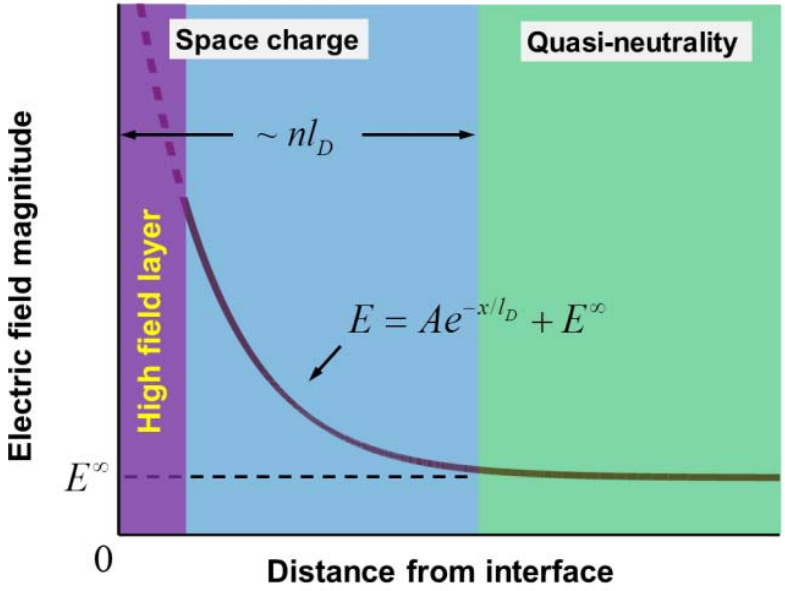

Schematic of the electric field near an interface with a decaying screening term plus a permanent remnant term .

Electric Field in a Growing Oxide Film

Two dominant representations:

- Homogeneous electric field across the film
- Electric field decays to zero exponentially away from the surface/interface assuming thermodynamic equilibrium

$$J_i = -D_i \nabla c_i + \varpi_i \mathbf{E} c_i \quad \text{Flux equations}$$

$$\varepsilon \nabla \bullet \mathbf{E} = \sum_i z_i e N_A c_i \quad \text{Linearized Poisson Boltzmann}$$

- Two negatively charged transporting species with identical valences (i.e. z1=z2=-1), e.g. electrons and interstitial anions
- Assume coupled-current condition

$$E = Ae^{-x/l_D} + E^o$$

$$E^o = \frac{k_B T}{e\bar{c}} \frac{D_1 - D_2}{D_1 D_2} J^o$$

$$l_D = \sqrt{\varepsilon k_B T / N_A e^2 \bar{c}}$$

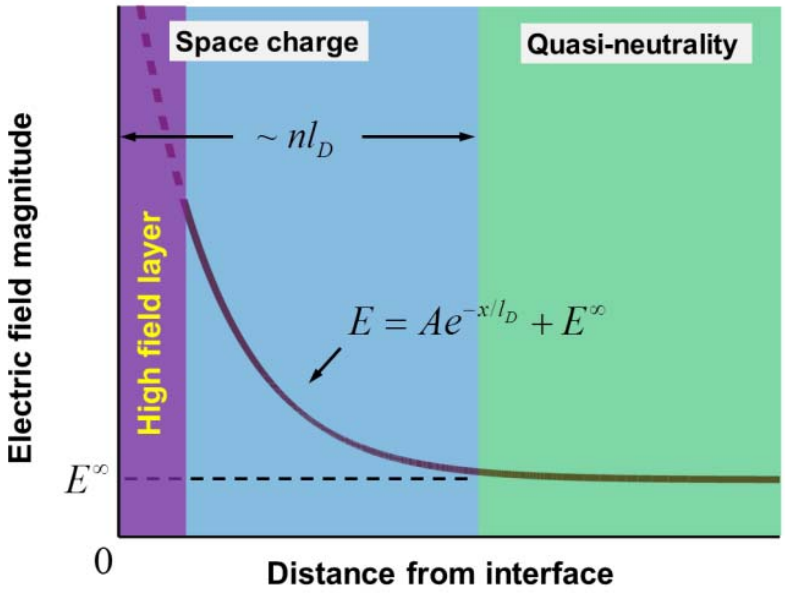

Schematic of the electric field near an interface with a decaying screening term plus a permanent remnant term in the bulk. Quasi-steady-state ionic diffusion with zero net electric current.

Unified understanding for the electric field from the viewpoints of kinetics and thermodynamics

Electric Field in a Growing Oxide Film

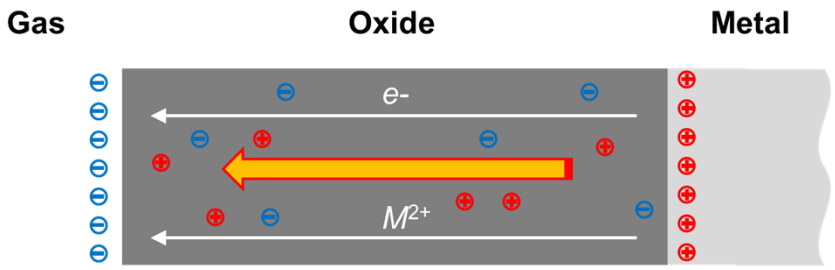

$$Z_1 \neq Z_2$$

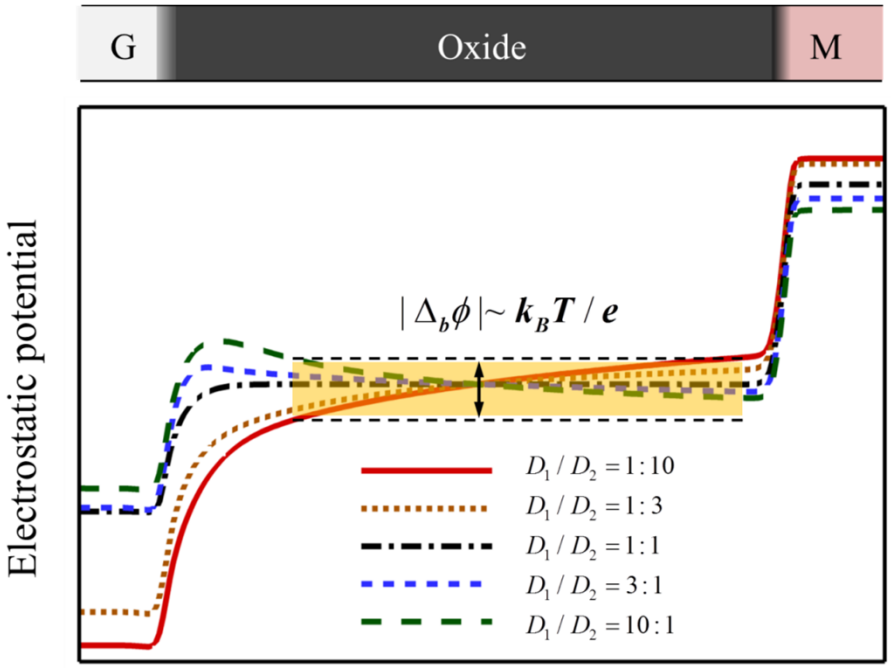

Simulated electrostatic potential profiles with different defect mobility ratios.

Similar characteristics in the electric field is recovered via simulations:

- Maximum magnitude obtained when the mobilities of the diffusing species have large disparity
- Exactly zero when point defects have identical mobilities

Electric Field in a Growing Oxide Film

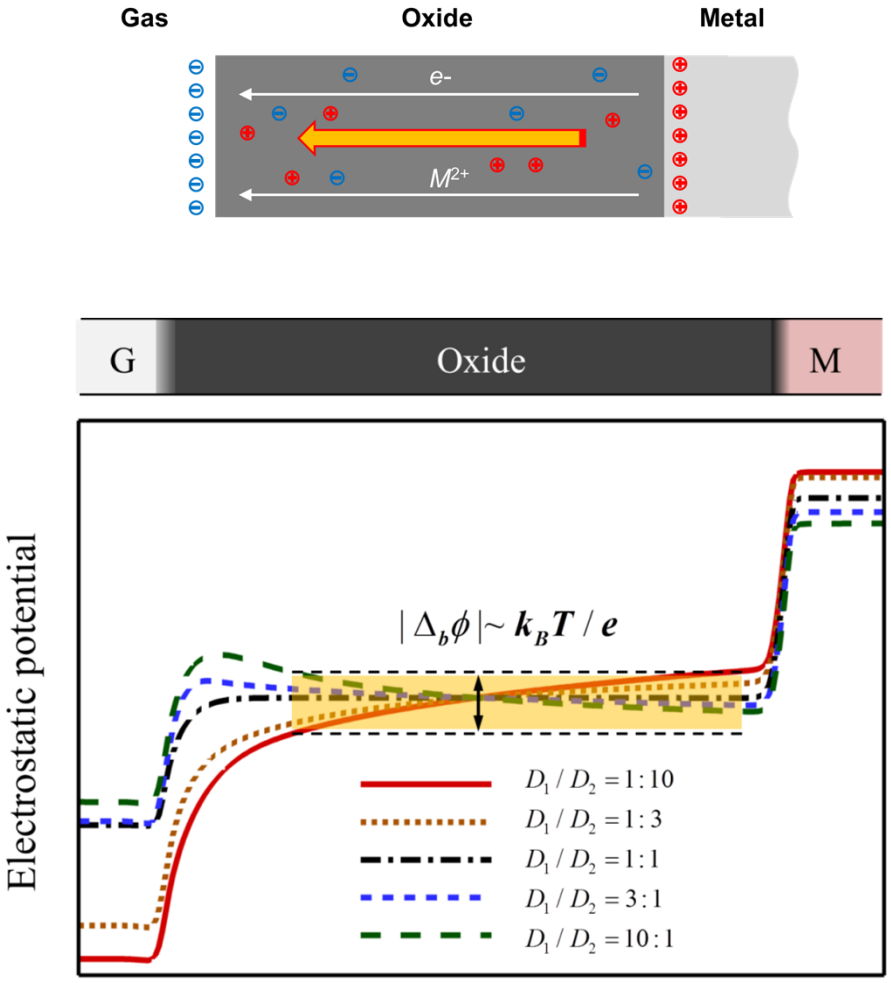

Simulated electrostatic potential profiles with different defect mobility ratios.

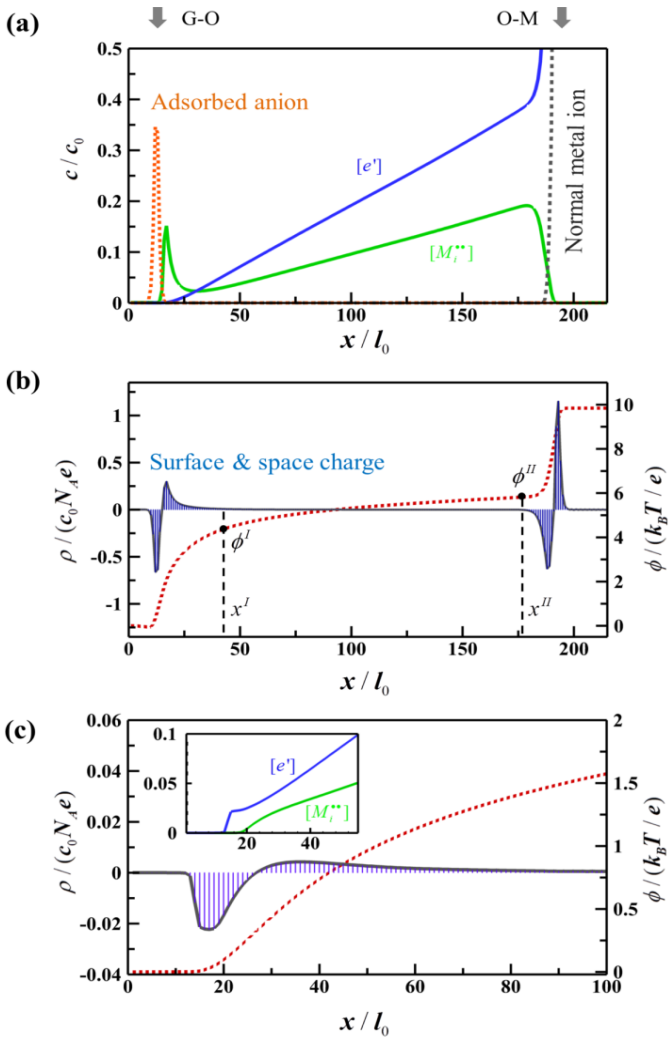

Representative simulated ionic diffusion in an oxide film. (a) Defect concentration; (b) charge and electrostatic potential distribution; (c) charge distribution without permanent surface charge.

Electric Field in a Growing Oxide Film

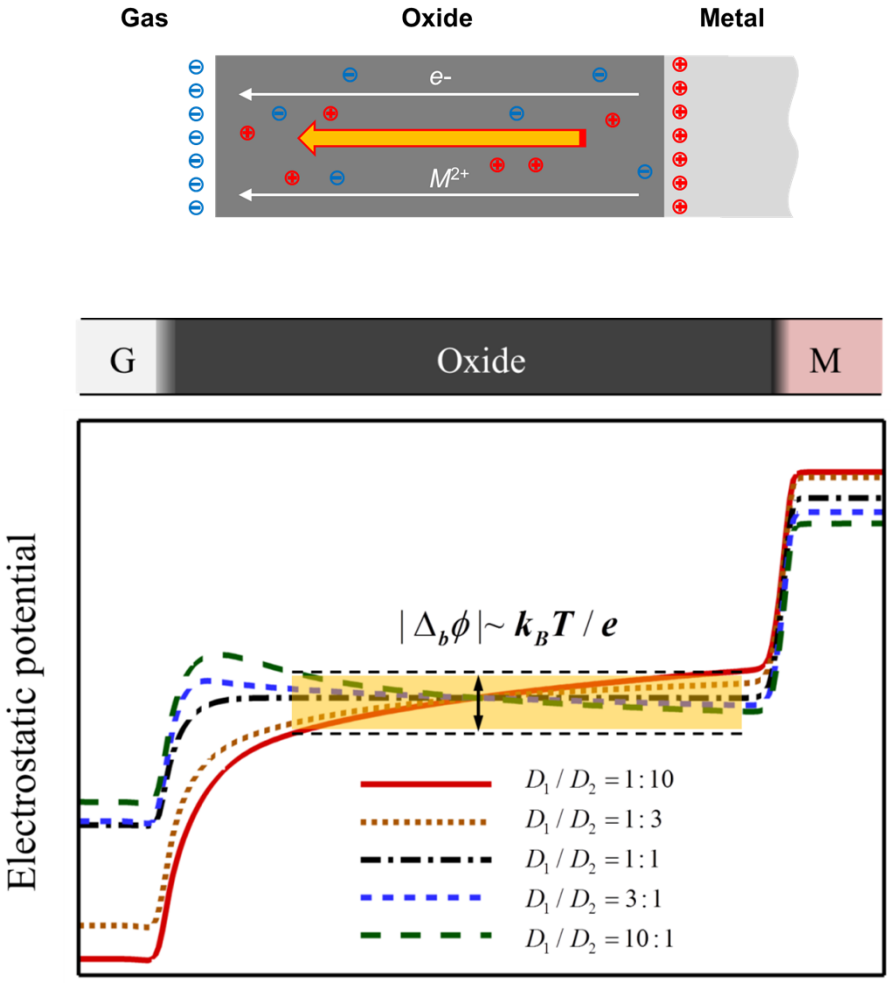

Simulated electrostatic potential profiles with different defect mobility ratios.

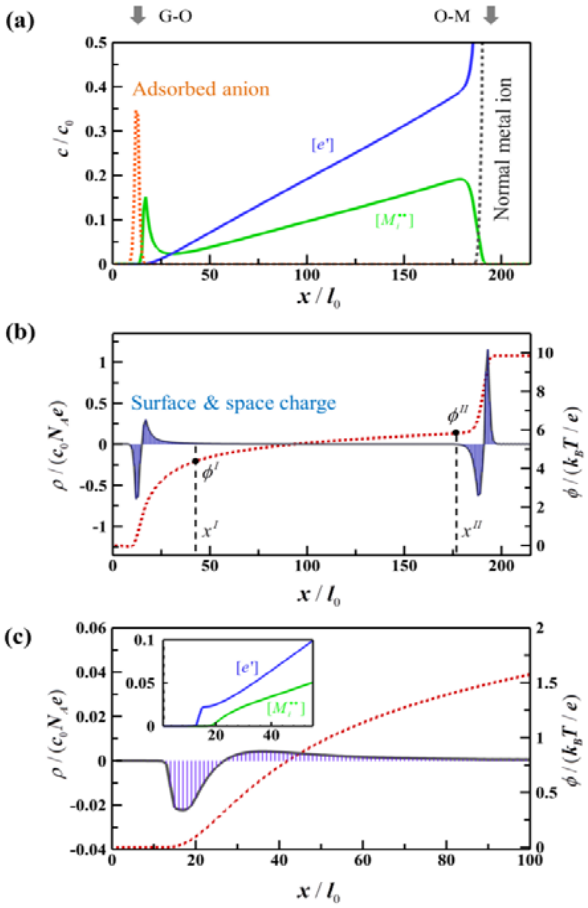

Representative simulated ionic diffusion in an oxide film. (a) Defect concentration; (b) charge and electrostatic potential distribution; (c) charge distribution without permanent surface charge.

Cheng and Wen, J. Phys. Chem. Lett. 5 (2014), 2289-2294

Efficient Algorithm to Solve Electrostatic Problems

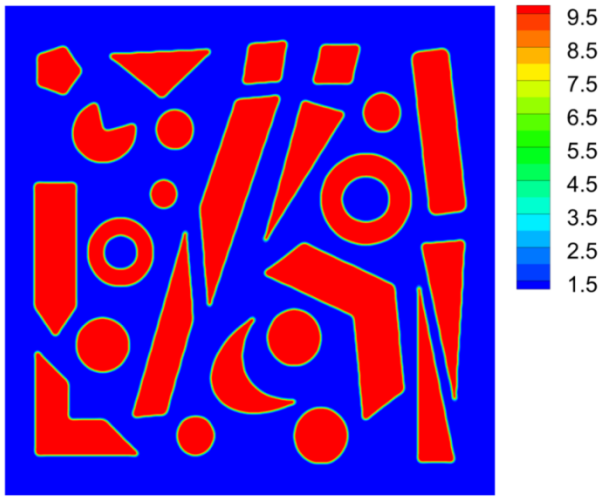

Dielectric constant distribution

External field

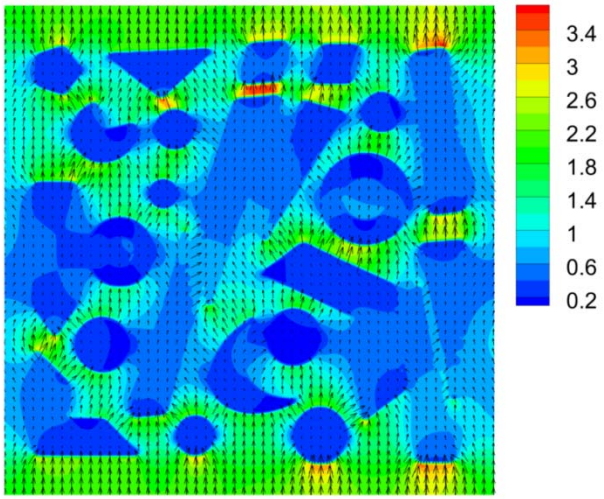

Actual electric field distribution

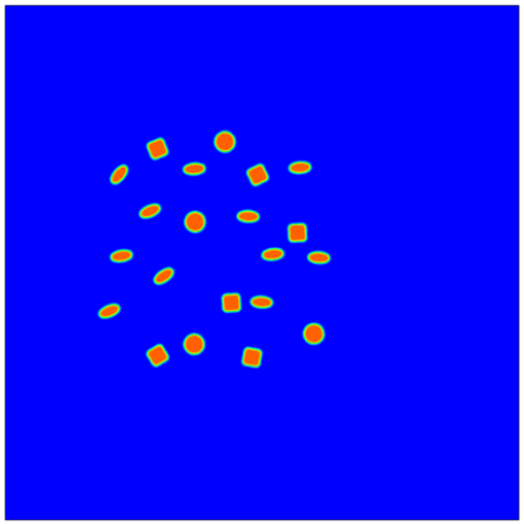

Nonuniform external field

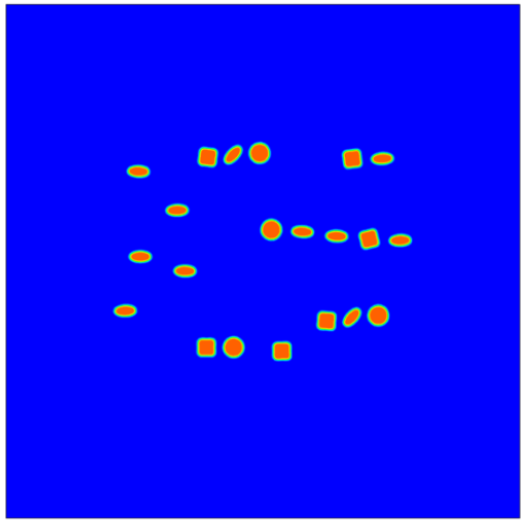

Dielectrophoresis process with various inter-particle force and hydrodynamic effects

Efficient Algorithm to Solve Electrostatic Problems

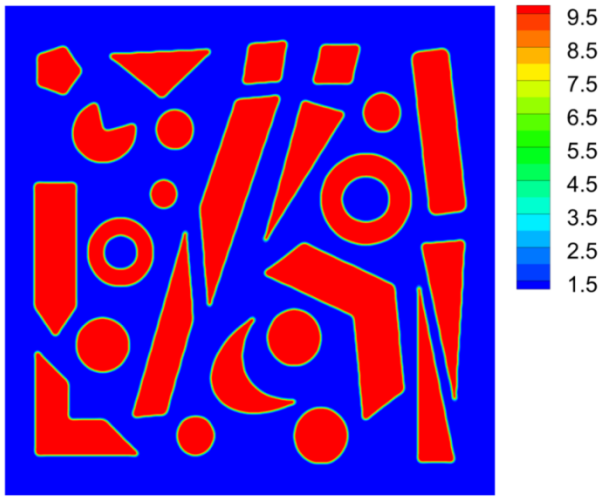

Dielectric constant distribution

External field

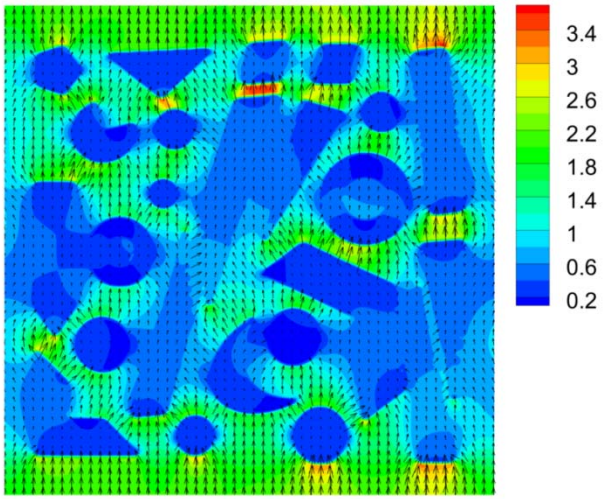

Actual electric field distribution

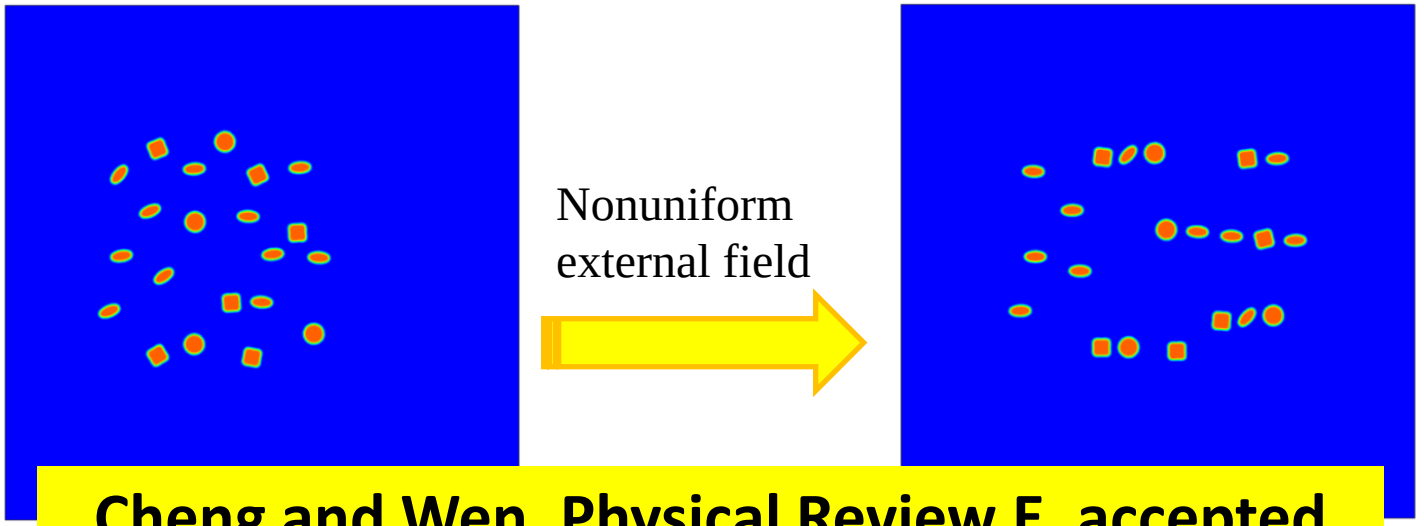

Cheng and Wen, Physical Review E, accepted

Dielectrophoresis process with various inter-particle force and hydrodynamic effects

On-going Efforts
Grain/phase boundaries in ionic solids

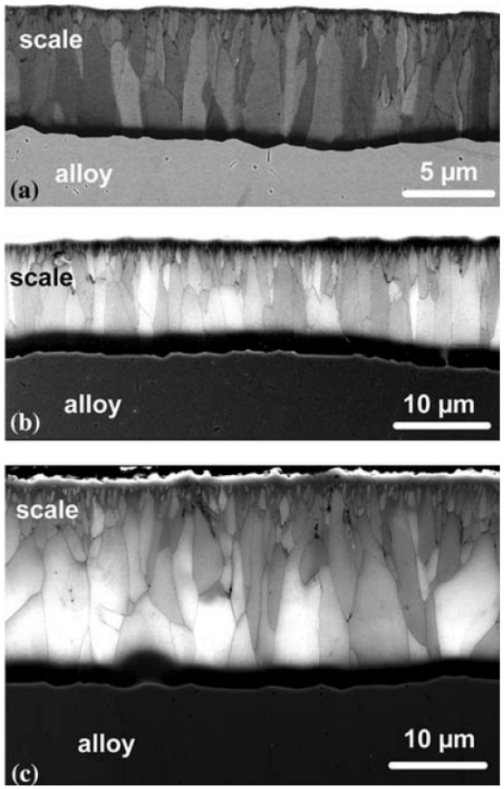

Alumina scales formed on the FeCrAlY alloy after air oxidation for (a) 100 hr (b) 500 hr, and (c) 2000 hr at 1200°C *(B. Gleeson et al, 2007)*

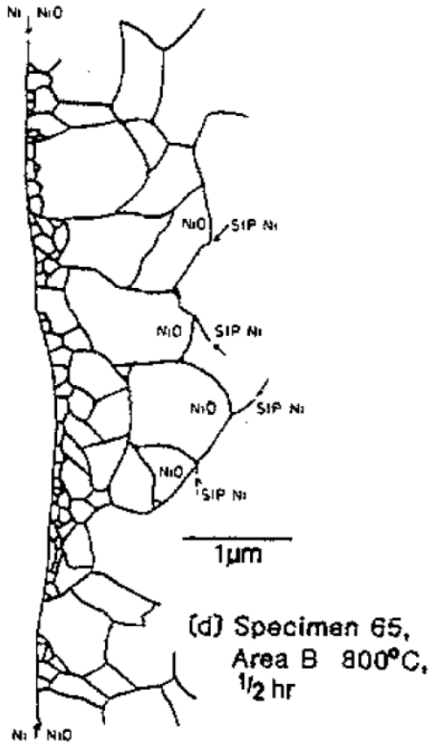

Grain boundary network of NiO formed on pure Ni substrate after air oxidation for at 800°C *(H. Atkinson, 1987)*

Microstructure effect on Kinetics

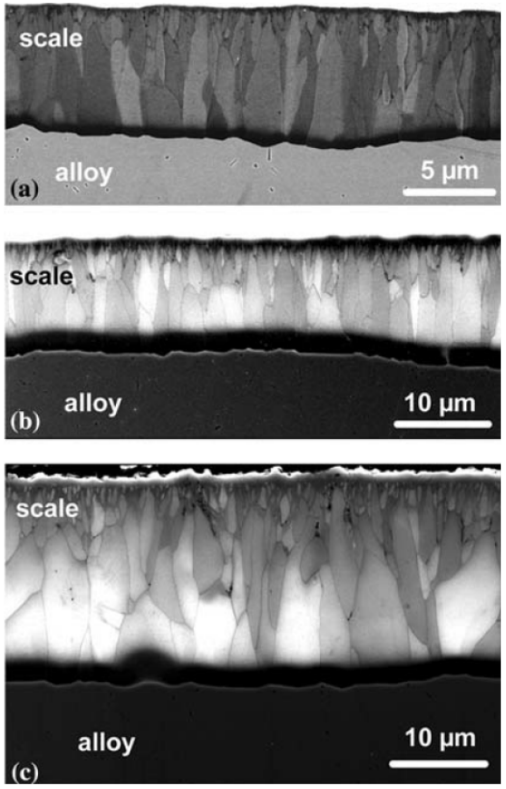

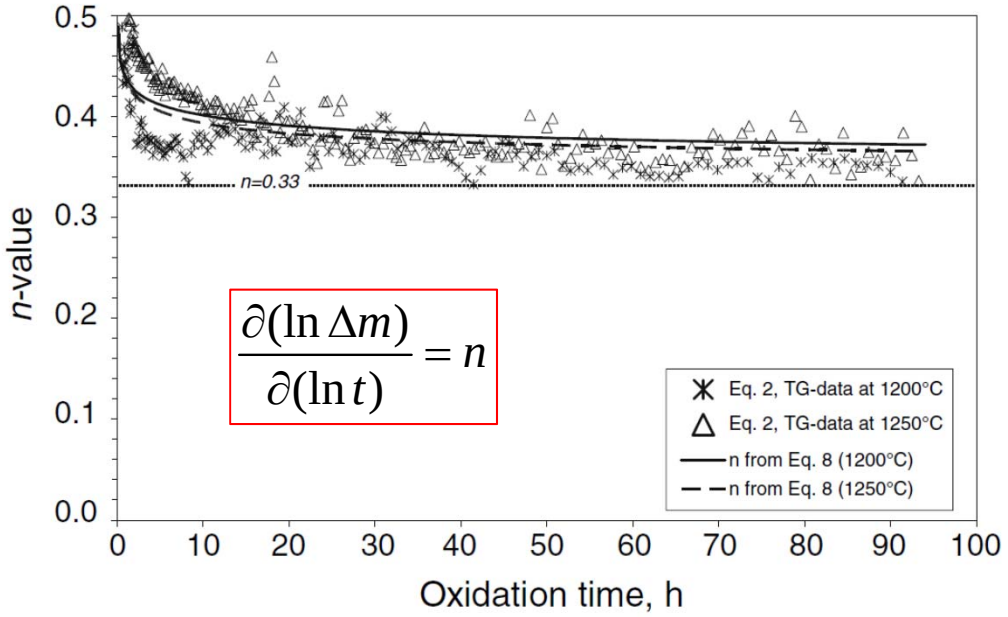

State-of-the-art in GB modeling

The effective diffusivity of ions in a polycrystalline is often described as

$$D_{eff} = D + 2D'\delta/g$$

- **Reflect no GB-diffusion mechanism; difficult to interface with ab initio (atomic level) calculations, and this model is often difficult to characterize the GB-diffusion properties of metal oxides.**
- **The activation energy of Al2O3 is inconsistent with traditional understanding on GB diffusion.**

For metals the activation energy of GB-diffusion is about half of lattice diffusion, but for Al2O3 the apparent activation energy of GB-diffusion is even above lattice diffusion. ***(A. Heuer, 2013)***

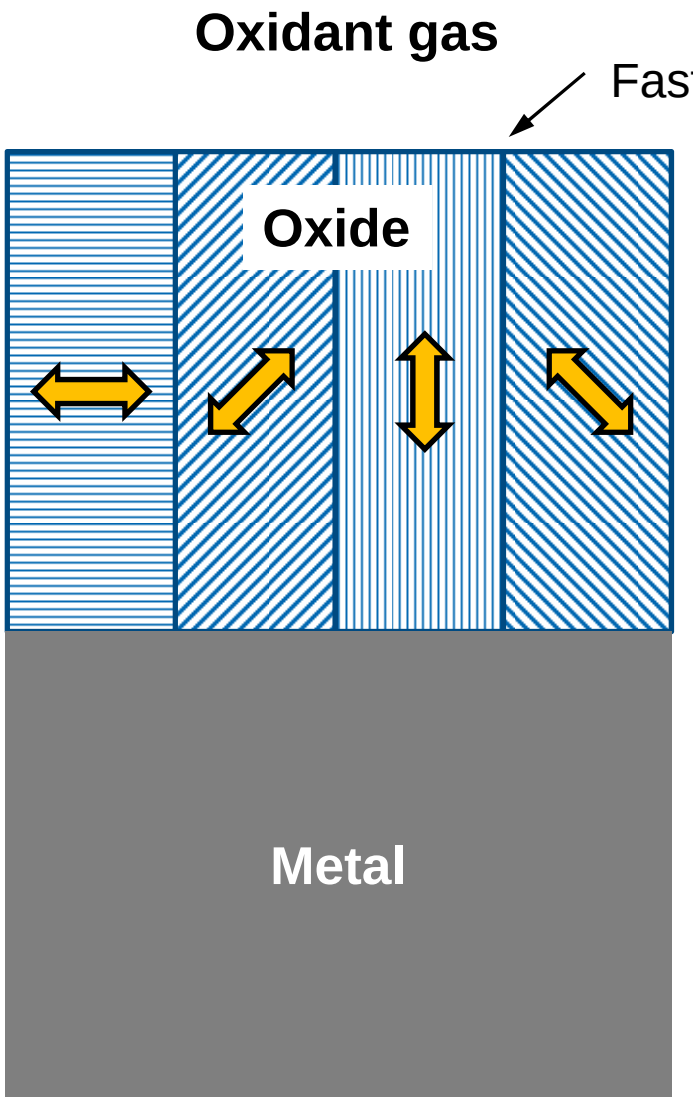

$$\begin{Bmatrix} P_1 \\ P_2 \end{Bmatrix} = \varepsilon_0 \begin{bmatrix} \chi_{11} & \chi_{12} \\ \chi_{21} & \chi_{22} \end{bmatrix} \begin{Bmatrix} E_1 \\ E_2 \end{Bmatrix}$$

$$\partial_i [\delta_{ij} + \chi_{ij}(\mathbf{r})] E_j(\mathbf{r}) = \rho_f(\mathbf{r}) / \varepsilon_0$$

↓

BCSA algorithm

Cheng, T.-L., Wen, Y.-H., Phys. Rev. E (accepted)

Preliminary simulation result: electric field distortion in a polycrystalline oxide

Textured dielectric (oxide) film with different crystallographic orientations (assuming 4 columnar grains)

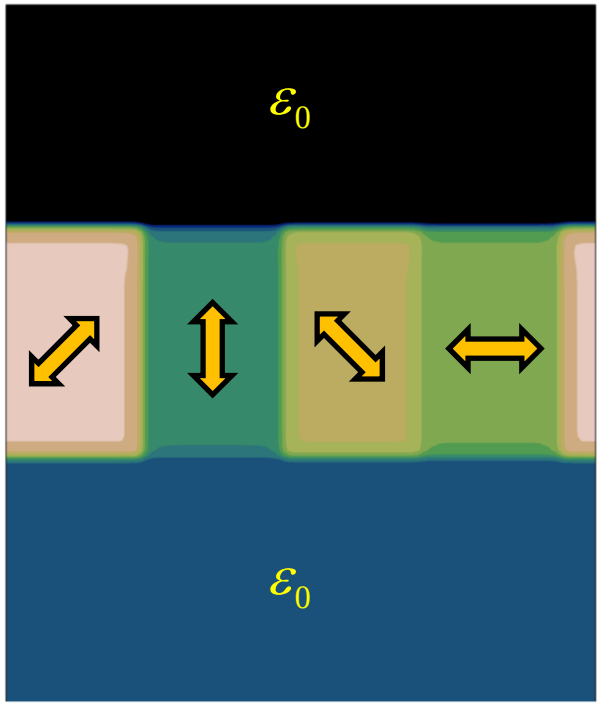

Bound charge distribution and electric field distribution in the presence of dielectric heterogeneity/anisotropy

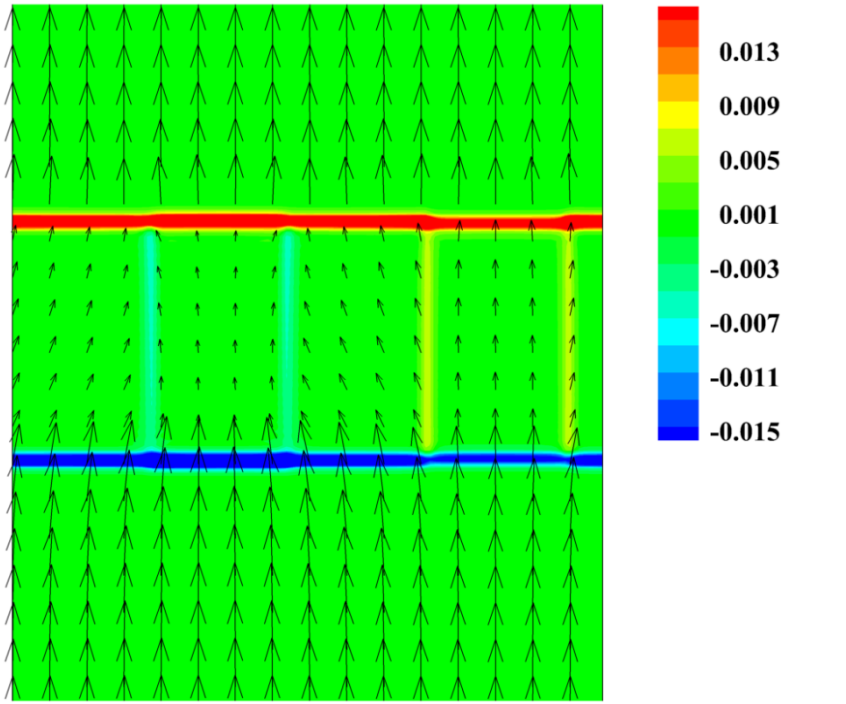

$E^{ex}=0.1E_0$

$$\begin{bmatrix} \chi_{11} & \chi_{12} \\ \chi_{21} & \chi_{22} \end{bmatrix} = \begin{bmatrix} \cos\theta & -\sin\theta \\ \sin\theta & \cos\theta \end{bmatrix} \begin{bmatrix} \chi_1^0 & 0 \\ 0 & \chi_2^0 \end{bmatrix} \begin{bmatrix} \cos\theta & \sin\theta \\ -\sin\theta & \cos\theta \end{bmatrix}, \quad \chi_1^0 = 4, \chi_2^0 = 1$$

Physics-based GB Modeling in Ionic Solids

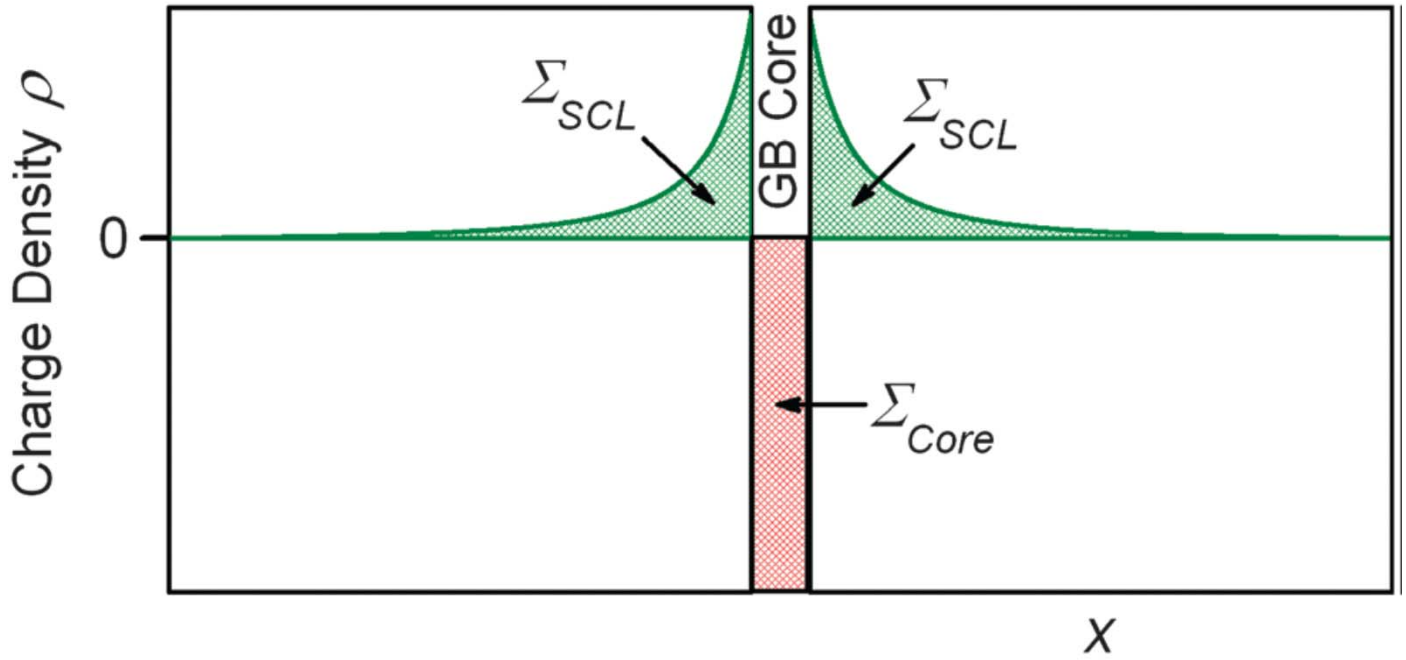

Schematic of charge distribution around a grain boundary of ionic crystal (J. Maier *et al*, *PCCP*, 2014)

Reactive element effects in oxidation:

Addition of small amount of reactive elements (Y, Hf, Zr, etc) may significantly change ionic transport and oxidation kinetics but the underlying mechanism is still in debate. This model may provide some new insights.

On-going Efforts
Linking DFT/MD and Phase-field Modeling

Input from DFT/MD

- point defect mobility along GBs and bulk lattice in oxides
- equilibrium defect concentration in bulk lattice and at GBs
- grain structure from experiments

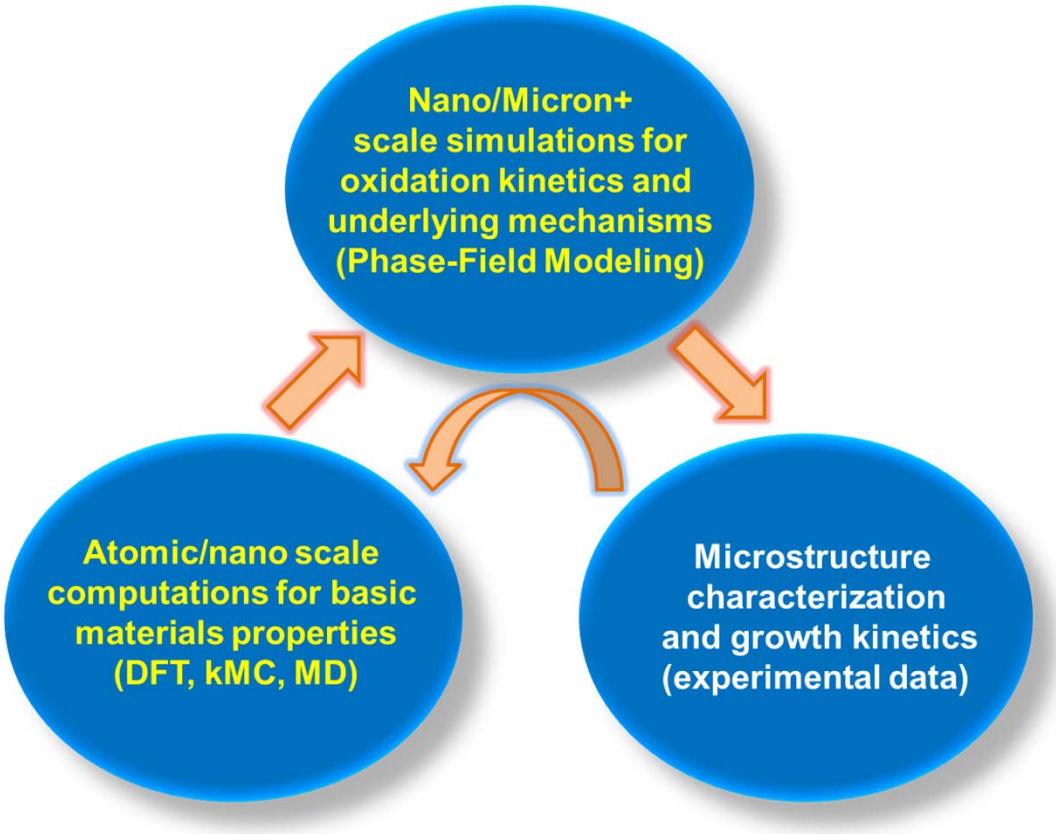

Specific problems:
(a) transport properties of oxide scale with complex grain structure
(b) grain growth in the oxide scale
(c) correlation between grain structure evolution and oxidation kinetics

Potential Application in Solid Oxide Fuel Cell

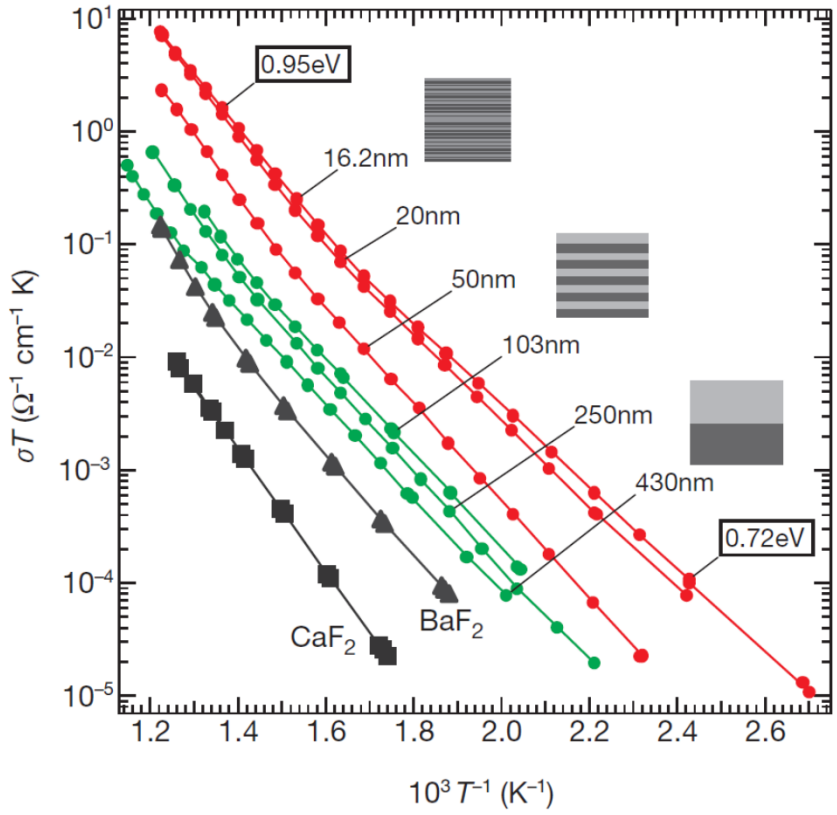

Space charge effect on Ionic conductivity of films with different interfacial density (period) (CaF_2/BaF_2 periodic heterostructure)

(N. Sata *et al*, *Nature*, 2000)

Summary of Oxidation Kinetics Modeling Task

- Developed a ***multiscale simulation capability*** based on Phase-Field Method to solve the complex coupling problem that involves transport of charged ions subject to interfacial reactions and long range electrostatic interactions

- Developed an ***efficient numerical algorithm*** to solve the charge interaction problem with arbitrary heterogeneity in electric properties

- Further development of the model is necessary to advance this model into a useful tool that can be used to predict the life of a complex alloy

Accomplishments

Peer-reviewed Journal publications:

1. Tianle Cheng and **Youhai Wen**, "Efficient bound charge successive approximation algorithm for solving electrostatics in complex and evolving dielectric heterostructures," **Phys. Review E**, 2015, accepted
2. Zhenyu Xing, et al., Reducing CO2 to Dense Nanoporous Graphene by Mg/Zn for High Power Electrochemical Capacitors. **Nano Energy**, 11(2015), p. 600
3. Tian-Le Cheng and **Youhai Wen**, "Toward a quantitative understanding of the electric field in thermal metal oxidation and a self-consistent Wagner theory," **J. Phys. Chem. Letters**, 2014, 5, 2289-2294
4. Tian-Le Cheng, **Youhai Wen** and Jeffrey A. Hawk, 'Diffuse-interface modeling and multiscale-relay simulation of metal oxidation kinetics - with revisit on Wagner's theory,' **J. Phys. Chem. C**, 2014, 118, 1269-1284
5. N. Wang, **Youhai Wen** and L.Q. Chen, "Pinning force from multiple second-phase particles in grain growth," **Computational Mater. Sci**., 2014, 93, 81-85
6. Nan Wang, **Youhai Wen** and Long-Qing Chen, "Pinning of grain boundary migration by a coherent particle," **Phil. Mag. Lett**. 94(2014), p.794

Article in Conference Proceedings

1. **Youhai Wen**, Tianle Cheng, Paul D. Jablonski, John Sears, and Jeffrey A. Hawk, "Stability of Gamma Prime in H282: Theoretical and Experimental Consideration," Proceedings of 8th Inter. Symp. On Superalloy 718 & Derivatives, 2014

Accomplishments

Conference Presentations:

1. **Youhai Wen**, “Electrochemistry based computational modeling of oxidation kinetics," 248th ACS National Meeting, San Francisco, CA, Aug. 10-14, 2014. **Invited.**
2. **Youhai Wen**, “Phase-field modeling of oxidation behavior," The 3rd International Symposium on Phase-Field Method, State College, PA, Aug. 26-29, 2014. **Invited.**
3. Tianle Cheng, **Youhai Wen**, and Jeffrey Hawk, “Diffuse Interface Modeling on Thermal Oxidation of Metals,” TMS 2014 Annual Meeting, San Diego, CA, Feb 16-20, 2014.
4. **Youhai Wen**, “Phase field modeling of metal oxidation behavior," MRS 2014 Spring Meeting, San Francisco, CA, April 21-25, 2014.
5. Tianle Cheng and **Youhai Wen**, ‘An Efficient Phase Field Model for Electrostatics in Complex Dielectric Heterostructures,’ 225th Electrochemical Society Meeting, Orlando, FL, May 11-15, 2014
6. Tianle Cheng, **Youhai Wen** and Jeffrey Hawk, ‘Diffuse Interface Modeling and Multi-Scale Relay Simulation of Thermal Oxidation of Metals,’ 225th Electrochemical Society Meeting, Orlando, FL, May 11-15, 2014
7. **Youhai Wen**, Jeffrey Hawk and David Alman, “Predicting Microstructural Stability for Advanced FE Systems,” 2014 NETL Crosscutting Research Review Meeting, Pittsburgh, PA, May 19-23, 2014.
8. Nan Wang, **Youhai Wen** and Longqing Chen, “Study of precipitate coherency loss and coherent strain effect in particle pinning using phase-field-crystal model,” The 3rd International Symposium on Phase-Field Method, State College, PA, Aug. 26-29, 2014.
9. **Youhai Wen**, Tianle Cheng, Paul D. Jablonski, John Sears, and Jeffrey A. Hawk, “Stability of Gamma Prime in H282: Theoretical and Experimental Consideration,” The 8th Inter. Symp. On Superalloy 718 & Derivatives, Pittsburgh, PA, Sep 28 – Oct 1, 2014.

Roadmap to Oxidation Modeling

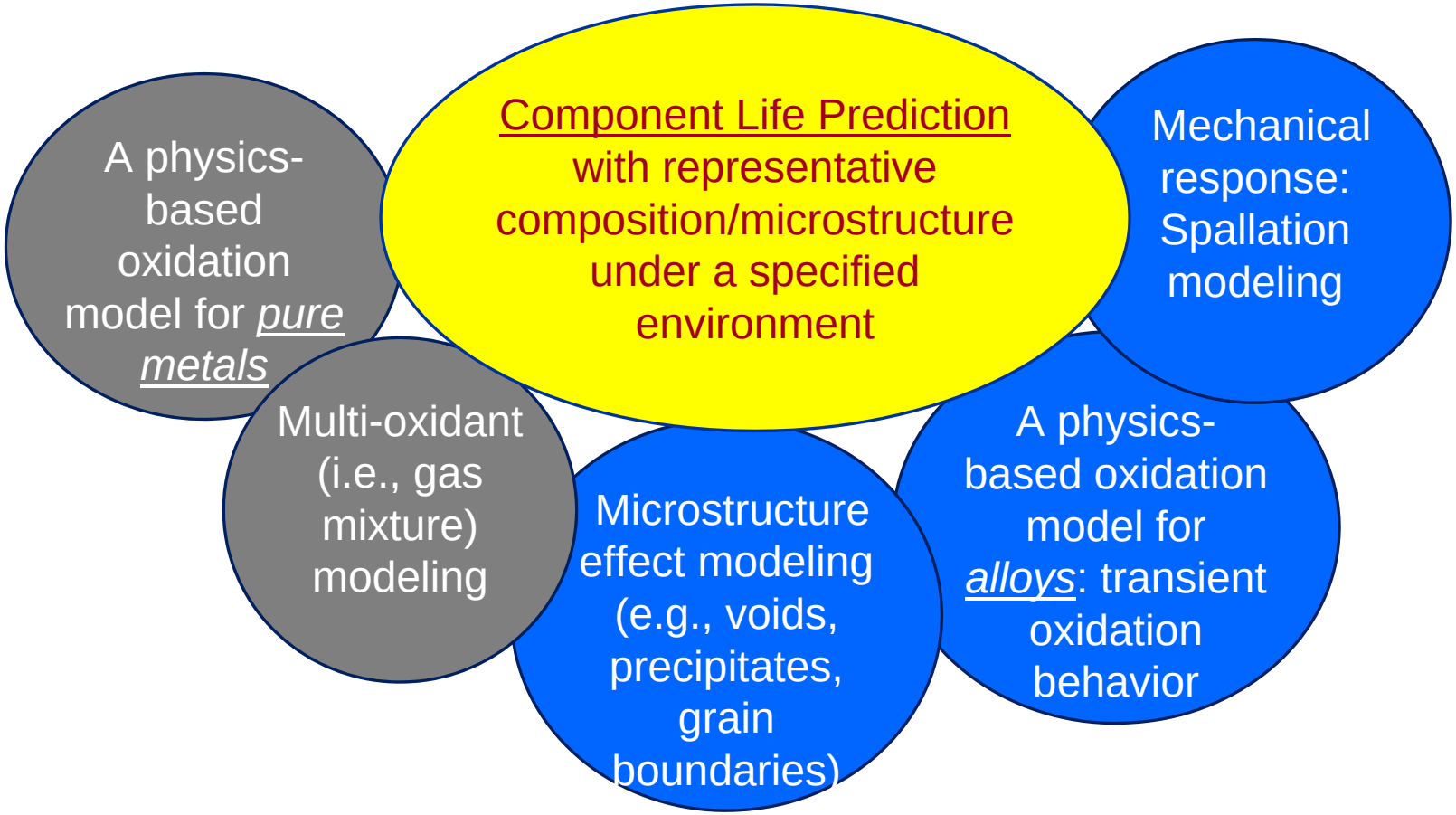

Phase-Field Method

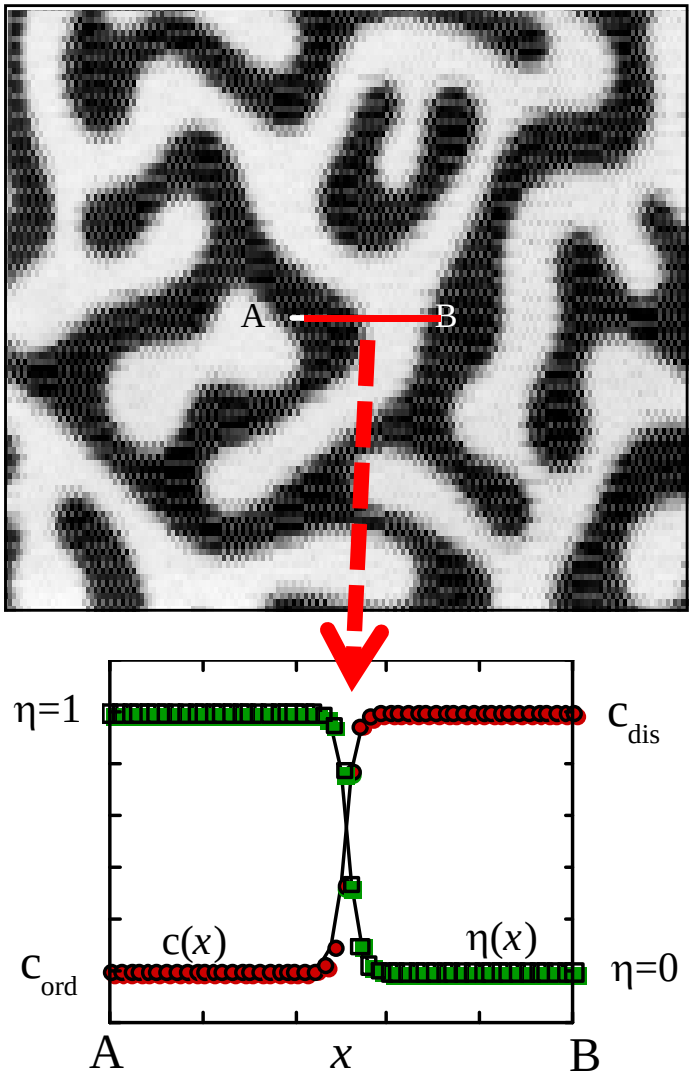

- Complex microstructure represented by finite set of field variables
- Diffused interface (vs sharp interface in front tracking methods)

$$F = \int_V \left\{ f_{ch}(c,\eta,T) + \left[\frac{1}{2}\kappa_c(\nabla c)^2 + \frac{1}{2}\kappa_\eta(\nabla \eta)^2 \right] + F_{el} \right\} dV$$

$$\frac{\partial \eta}{\partial t} = -L\left(\frac{\delta F(c,T,\eta)}{\delta \eta}\right) + \varsigma_\eta$$

$$\frac{\partial c}{\partial t} = M\nabla^2\left(\frac{\delta F(c,T,\eta)}{\delta c}\right) + \varsigma_c$$

(Ginzburg-Landau, Cahn-Hilliard)

Table 1. Simulated $\Delta_b\phi$ dependence on increasing surface potential $\Delta\phi_{OG} = \phi^I - \phi_G$, with change in the amount of prescribed surface charge

$\Delta\phi_{OG} / (k_B T / e)$	0.98	2.02	4.00	5.96	8.02
$\Delta_b\phi / (k_B T / e)$	1.13	1.22	1.21	1.22	1.23

Table 2. Simulated dependence of $\Delta_b\phi$ on total oxide film thickness.

L / l_D^*	40	80	160	320	480	640
$\Delta_b\phi / (k_B T / e)$	0.88	1.21	1.66	2.07	2.18	2.23

The bulk electrostatic potential drop is insensitive to the surface charge and film thickness